UNCLASSIFIED

CENTRAL RESEARCH LIBRARY
DOCUMENT COLLECTION

MARTIN MARIETTA ENERGY SYSTEMS LIBRARIES

3 4456 0350434 9

ORNL-2207
Engineering cy. 138

SPHERICAL SEGMENT WITH CIRCULAR HOLE AT VERTEX LOADED AXISYMMETRICALLY ALONG THE EDGES

APPENDIX A

AXIALLY LOADED CIRCULAR CYLINDER ATTACHED TO SPHERICAL SHELL

F. J. Stanex

LIBR

DO NOT T ERSON

If you wish someone else to see this document send in name with document and the library will arrange a loan

OAK RIDGE NATIONAL LABORATORY
OPERATED BY
UNION CARBIDE NUCLEAR COMPANY
A Division of Union Carbide and Carbon Corporation
UCC
POST OFFICE BOX X · OAK RIDGE, TENNESSEE

UNCLASSIFIED

Printed in USA. Price 35 cents. Available from the

Office of Technical Services
U. S. Department of Commerce
Washington 25, D. C.

LEGAL NOTICE

This report was prepared as an account of Government sponsored work. Neither the United States, nor the Commission, nor any person acting on behalf of the Commission:

A. Makes any warranty or representation, express or implied, with respect to the accuracy, completeness, or usefulness of the information contained in this report, or that the use of any information, apparatus, method, or process disclosed in this report may not infringe privately owned rights; or

B. Assumes any liabilities with respect to the use of, or for damages resulting from the use of any information, apparatus, method, or process disclosed in this report.

As used in the above, "person acting on behalf of the Commission" includes any employee or contractor of the Commission to the extent that such employee or contractor prepares, handles or distributes, or provides access to, any information pursuant to his employment or contract with the Commission.

UNCLASSIFIED

138

ORNL-2207

Contract No. W-7405-eng-26

Aircraft Reactor Experimental Engineering Division

SPHERICAL SEGMENT WITH CIRCULAR HOLE AT VERTEX LOADED AXISYMMETRICALLY ALONG THE EDGES

APPENDIX A

AXIALLY LOADED CIRCULAR CYLINDER ATTACHED TO SPHERICAL SHELL

By

FLOYD J. STANEK

DATE ISSUED

DEC 19 1956

OAK RIDGE NATIONAL LABORATORY
Operated By
CARBIDE AND CARBON CHEMICALS COMPANY
A Division of Union Carbide and Carbon Corporation
Post Office Box X
Oak Ridge, Tennessee

UNCLASSIFIED

MARTIN MARIETTA ENERGY SYSTEMS LIBRARIES

3 4456 0350434 9

INTERNAL DISTRIBUTION

1. R. G. Affel
2. C. J. Barton
3. M. Bender
4. D. S. Billington
5. F. F. Blankenship
6. E. P. Blizard
7. C. J. Borkowski
8. W. F. Boudreau
9. G. E. Boyd
10. M. A. Bredig
11. W. E. Browning
12. F. R. Bruce
13. A. D. Callihan
14. D. W. Cardwell
15. C. E. Center (K-25)
16. R. A. Charpie
17. C. E. Clifford
18. J. H. Coobs
19. W. B. Cottrell
20. D. D. Cowen
21. S. J. Cromer
22. R. S. Crouse
23. F. L. Culler
24. J. H. DeVan
25. L. M. Doney
26. D. A. Douglas
27. E. R. Dytko
28. W. K. Eister
29. L. B. Emlet (K-25)
30. D. E. Ferguson
31. A. P. Fraas
32. J. H. Frye, Jr.
33. W. T. Furgerson
34. E. J. Breeding
35. W. R. Grimes
36. E. E. Hoffman
37. H. W. Hoffman
38. A. Hollaender
39. A. S. Householder
40. J. T. Howe
41. W. H. Jordan
42. G. W. Keilholtz
43. C. P. Keim
44. M. T. Kelley
45. F. Kertesz
46. E. M. King
47. J. A. Lane
48. R. B. Lindauer
49. R. S. Livingston
50. R. N. Lyon
51. F. C. Maienschein
52. W. D. Manly
53. E. R. Mann
54. L. A. Mann
55. W. B. McDonald
56. F. R. McQuilkin
57. R. V. Meghreblian
58. R. P. Milford
59. A. J. Miller
60. R. E. Moore
61. J. G. Morgan
62. K. Z. Morgan
63. J. P. Murray (Y-12)
64. M. L. Nelson
65. G. J. Nessle
66. R. B. Oliver
67. L. G. Overholser
68. P. Patriarca
69. R. W. Peelle
70. A. M. Perry
71. J. C. Pigg
72. H. F. Poppendiek
73. D. H. Platus
74. A. E. Richt
75. M. T. Robinson
76. H. W. Savage
77. A. W. Savolainen
78. R. D. Schultheiss
79. E. D. Shipley
80. A. Simon
81. O. Sisman
82. J. Sites
83. M. J. Skinner
84. G. P. Smith
85. A. H. Snell
86. C. D. Susano
87. J. A. Swartout
88. E. H. Taylor
89. R. E. Thoma
90. D. B. Trauger
91. E. R. Van Artsdalen
92. G. M. Watson
93. A. M. Weinberg
94. D. L. Platus

95-104. F. J. Stanek
105. B. L. Greenstreet
106. S. E. Moore
107. D. M. Miller
108. J. R. Tallackson
109. F. A. Field
110. J. C. White
111. G. D. Whitman
112. J. C. Wilson
113. E. P. Wigner (consultant)
114. C. E. Winters
115-116. ORNL - Y-12 Technical Library, Document Reference Section
117-136. Laboratory Records Department
137. Laboratory Records, ORNL R.C.
[redacted]-139. Central Research Library

EXTERNAL DISTRIBUTION

140. Chester Biglow, Pratt and Whitney Aircraft (Fox Project)
141. Arthur Chalfant, Pratt and Whitney Aircraft (Fox Project)
142-145. R. L. Maxwell, University of Tennessee
146. R. F. Bacher, California Institute of Technology
147. Division of Research and Development, AEC, ORO
148-723. Given distribution as shown in TID-4500 under Engineering category (200 copies - OTS)

TABLE OF CONTENTS

	Page
Index to Tables and Figures	v
Acknowledgement	1
Nomenclature	2
Introduction	3
Basic Equations of the Classical Theory	5
The Classical Theory	5
Results: Case I	9
Case II	21a
Tables of Functions	10
Discussion of Results	27
Conclusions	27
Appendix A	29
Procedure	29
Results	32
Discussion of Results	38
Conclusions	39

INDEX TO TABLES AND FIGURES

SPHERICAL SEGMENT WITH CIRCULAR HOLE AT VERTEX LOADED AXISYMMETRICALLY ALONG THE EDGES

	Title	Page
Fig. 1	Spherical segment with general loading at inner and outer edges	4
Table I	Q and Q cot ϕ	10
Table II	Q' and V	11
Table III	M_ϕ and M_θ	12
Fig. 2a,b,c	Radial displacements - Case I	13
	(a) Due to shearing force, Q_α (b) Due to normal force, N_α (c) Due to shearing force, Q_β	
Fig. 2d,e	Radial displacements (dimensionless)	14
	(d) Due to bending moments, M_α (e) Due to bending moments, M_β	
Fig. 3-4	Meridional membrane stresses, $\sigma_{\phi,m}$, for Case I - General Loading; Fig. 3, due to shearing forces Q_α and Q_β, Fig. 4, due to normal force N_α and bending moments, M_α and M_β	15
5	Meridional bending stresses, outside surface, $\sigma_{\phi,B}$, for Case I - General Loading; due to bending moments, M_α and M_β.	16
6	Meridional bending stresses, outside surface, $\sigma_{\phi,B}$, for Case I - General Loading, due to shearing forces Q_α and Q_β.	17
7	Circumferential membrane stresses, $\sigma_{\theta,m}$, for Case I - General Loading due to shearing forces, Q_α and Q_β	18
8	Circumferential membrane stresses, $\sigma_{\theta,m}$, for Case I - General Loading, due to normal force, N_α, and bending moments, M_α and M_β	19
9	Circumferential bending stresses, outside surface, $\sigma_{\theta,B}$, for Case I - General Loading due to shearing forces Q_α and Q_β . . .	20

Index to Tables and Figures (cont'd.)

	Title	Page
10	Circumferential bending stresses, outside surface, $\sigma_{\theta,B}$, for Case I - General Loading due to bending moments, M_α and M_β . . .	21
11	Radial displacements - Case II	22
	(a) Due to shearing force, Q_α (b) Due to bending moment, M_α (c) Due to normal force, N_α	
12	Meridional membrane stresses, $\sigma_{\theta,m}$, for Case II - Fixed Outer Edge, due to loads applied at inner edge	23
13	Meridional bending stresses, outside surface, $\sigma_{\theta,m}$, for Case II - Fixed Outer Edge, due to loads applied at inner edge. . . .	24
14	Circumferential membrane stresses, $\sigma_{\theta,m}$, for Case II - Fixed Outer Edge, due to loads applied at inner edge	25
15	Circumferential bending stresses, outside surface, $\sigma_{\theta,B}$, for Case II - Fixed Outer Edge, due to loads applied at inner edge. . . .	26

APPENDIX A

AXIALLY LOADED CIRCULAR CYLINDER ATTACHED TO SPHERICAL SHELL

	Title	Page
Fig. A1	Axially loaded circular cylinder connected to spherical shell	30
Table A1	Q" for $\phi = 5^\circ$ and 10°	30
Table A2	Summary of the Geometrical Dimensions for the Cases Considered.	32
Table A3	Partial Results	32
Fig. A2	Principal Meridional Stresses . . . . . (Theoretical and Experimental)	34
Fig. A3	Principal Circumferental Stresses . . . . . (Theoretical and Experimental)	35
Fig. A4	Principal Meridional Stresses for Case A4 . . .	36
Fig. A5	Principal Circumferential Stresses for Case A4	37

ACKNOWLEDGEMENT

The author wishes to take this opportunity to express his sincere appreciation and thanks to Professor R. L. Maxwell, College of Engineering, University of Tennessee, for providing the experimental results presented in this paper, prior to the completion of his formal report.

The author also wishes to thank C. A. Proaps for her help in checking and carrying out many of the numerous numerical calculations required for the completion of this report, and to W. R. Lockhard for his drawing of the numerous figures presented in this report.

NOMENCLATURE

a - radius of middle surface of shell

h - uniform thickness of shell

i - $\sqrt{-1}$

E - Young's Modulus of Elasticity

γ - Poisson's ratio

ϕ - angle in meridional direction, positive from the axis of symmetry

M - bending moment per unit length, positive increases curvature

N - normal force, per unit length, tension positive

Q - radial shear, per unit length

subscript ϕ - meridional direction

subscript θ - circumferential direction

2α - total central angle subtended by the circular hole, results are for $A = 5^{\circ}$

2β - total central angle subtended by outer edge of spherical segment, results are for $\beta = 45^{\circ}$

subscript α - inner edge of shell

subscript β - outer edge of shell

' - differentiation with respect to ϕ

v - tangential displacement in ϕ-direction

w - radial displacement, positive inward

σ_{ϕ} - stress in ϕ-direction

σ_{θ} - stress in θ-direction

INTRODUCTION

The purpose of this paper is to give the results of a stress analysis of a spherical segment with circular hole at the vertex which is loaded symmetrically with respect to its axis along the edges of the shell.

Results were obtained and are given in this paper for two cases.
Case I: General Loading, i.e., normal force, radial shearing force, and bending moment applied at each of the two edges of the shell (Figure 1).
Case II: General Loading at inner edge with outer edge rigidly fixed.

The classical, small-deflection theory of thin shells was used. This method, in short, involves the evaluation of four hypergeometric series and their deviratives which give the solution to a fourth order differential equation for the shearing force, Q_ϕ. The development of the classical theory is presented in Timoshenko's text, Theory of Plates and Shells.

The above problem is then extended by attaching an axially loaded circular cylinder to the inner edge of the shell. The manner in which this was done is shown in the appendix. Several cases were analyzed, and the results are summarized. The cases differ primarily in their relative geometrical dimensions and outer edge conditions. These differences are summarized in Table A-2 in the appendix.

The relative dimensions for Case A1 were selected, so as to coincide, as nearly as it was possible to do so, with a physical model from which the principal stresses were obtained experimentally. A comparison is then made between the theoretical and the experimental results, Figures A2 and A3. In general, the two results are in good agreement.

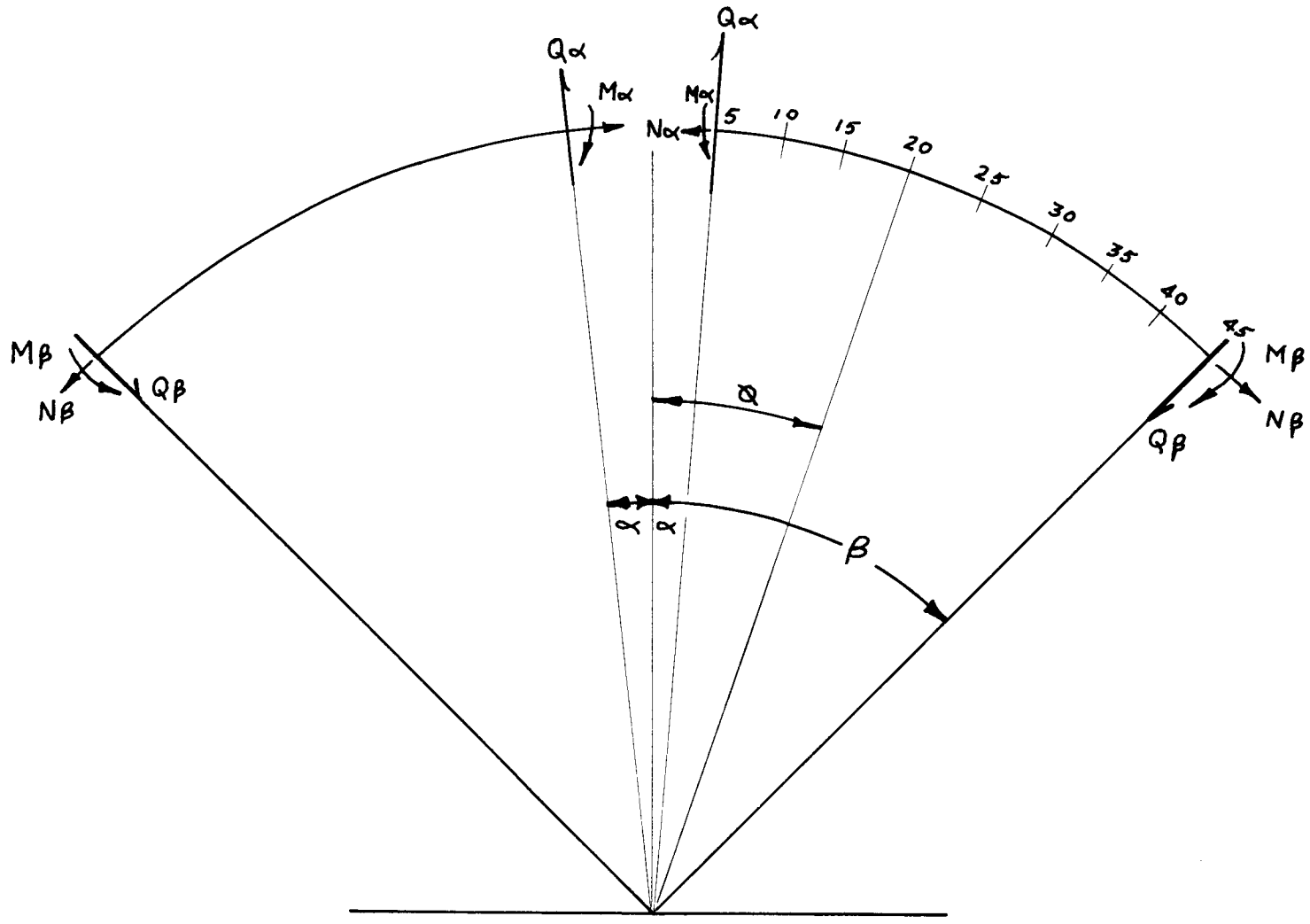

FIGURE 1: Spherical Segment with General Loading at Inner and Outer Edges.

UNCLASSIFIED
ORNL-LR-DWG. 16875

BASIC EQUATIONS OF THE CLASSICAL THEORY

Since $Q_\theta = 0$ because of symmetrical loading, the subscript ϕ on Q is hereafter ommitted.

I. Equilibrium equations.

$$(N'_\phi - Q)\tan\phi + N_\phi - N_\theta = 0$$

$$(N_\phi + N_\theta + Q')\tan\phi + Q = 0$$

$$(M'_\phi - Qa)\tan\phi + M_\phi - M_\theta = 0$$

II. The stress-strain relations (Hooke's Law) in terms of displacements.

$$N_\phi = \frac{Eh}{a(1 - \gamma^2)} \left[(v' - w) + \gamma\ (v\cot\phi - w) \right]$$

$$N_\theta = \frac{Eh}{a(1 - \gamma^2} \left[(v\cot\phi - w) + \gamma\ (v' - w) \right]$$

$$M_\phi = \frac{Eh^3}{12a^2(1 - \gamma^2)} \left[(v' + w'') + \gamma\ (v + w')\cot\phi \right]$$

$$M_\theta = \frac{Eh^3}{12a^2(1 - \gamma^2)} \left[(v + w')\cot\phi + \gamma\ (v' + w'') \right]$$

THE CLASSICAL THEORY

By making the substitution $V = v + w'$ and using V and Q as the dependent variables, the following differential equations are obtained:

$$Q'' - Q'\cot\phi - Q(\cot^2\phi - \gamma) = \frac{Eh}{a}\ V \qquad \text{IIIa}$$

$$V'' + V'\cot\phi - V(\gamma + \cot^2\phi) = \frac{-Q12a^3(1 - \gamma^2)}{Eh^3} \qquad \text{IIIb}$$

Substituting for V in IIIb, the expression IIIa, one obtains a fourth order differential equation for Q. This may be written as two second order differential equations in the following form:

$$Q'' + \cot\phi\, Q' - \cot^2\phi\, Q \pm 2i\, \delta^2\, Q = 0 \qquad 1.$$

where $$\delta^4 = \frac{a^2}{h^2}\; 3(1 - \gamma^2) - \frac{\gamma^2}{4}$$

By making the substitution

$$Q = z \sin\phi \text{ and } x = \sin^2\phi,$$

equation 1 becomes

$$x(x - 1)\, z_{xx} + (5x/2 - 2)z_x + (1 \pm 2i\delta^2)z/4 = 0 \qquad 2.$$

where the subscript denote differentiation with respect to x.

It can be shown that equation 2 has two solutions

$$z_1 = \sum_{n=0}^{\infty} A_n x^n$$

$$z_2 = z_1 \ln x + \frac{1}{x} \sum_{n=0}^{\infty} B_n x^n$$

A_n may be found by substituting several of the initial terms of z_1 in equation 2 and equating the coefficients of like powers of x to zero. Then by mathematical induction, we find

$$A_n = A_{n-1} \frac{2(n - 1)(2n + 1) + 1 - 2i\delta^2}{4n\,(n + 1)} \qquad n \geqslant 1$$

A_o may be any arbitrary constant except zero.

Similarly, by substituting several of the initial terms of z_2 in equation 2, we find

$$B_o = \frac{-4A_o}{1 + 2i\delta^2}$$

and

$$B_n = \frac{1}{n(n-1)} \left[\left(\frac{2(n-2)(2n-1) + 1 - 2i\delta^2}{4} \right) B_{n-1} + (2n - 5/2)A_{n-2} + (1 - 2n)A_{n-1} \right] \qquad n \geqslant 2$$

B_1 may be any arbitrary constant.

Since A_o and B_1 may be any arbitrary constant, they were both taken equal to 1.

By evaluating A_n and separating the real and imaginary parts of z_1 and substituting for z and x we obtain two series Q_1 and Q_2. Similarly, for z_2 we obtain Q_3 and Q_4. It can then be shown that the complete general equation for Q is

$$Q = C_1Q_1 + C_2Q_2 + C_3Q_3 + C_4Q_4 \qquad 3.$$

where C_j $(j = 1,2,3,4)$ are constants of integration.

It can also be shown that the complete general solution of V is

$$\begin{aligned} V &= C_1(\gamma Q_1 + 2\delta^2 Q_2) + C_2(\gamma Q_2 - 2\delta^2 Q_1) \\ &\quad + C_3(\gamma Q_3 + 2\delta^2 Q_4) + C_4(\gamma Q_4 - 2\delta^2 Q_3) \qquad 4. \\ &\equiv C_1 V_1 + C_2 V_2 + C_3 V_3 + C_4 V_4 \end{aligned}$$

Having the solutions for Q and V, one may obtain, after considerable algebric manipulation, the following relations:

$$M_\phi = \frac{-D}{a^2} \left[V\cot\phi + \gamma V' \right] \qquad 5.$$

$$M_\theta = \frac{-D}{a^2}\left[v' + \gamma V\cot\phi\right] \qquad 6.$$

$$N_\phi = K/\sin^2\phi - Q\cot\phi \qquad 7.$$

$$N_\theta = -K/\sin^2\phi - Q' \qquad 8.$$

$$v = \frac{a(1+\gamma)}{Eh}\left[K(\sin\phi \ln \tan\phi/2 - \cot\phi) + Q + C_o \sin\phi\right] \qquad 9.$$

$$w = \frac{a}{Eh}\left[K(1+\gamma)(\cos\phi \ln \tan\phi/2 + 1) - (N_\phi + N_\theta) + C_o (1+\gamma)\cos\phi\right] \qquad 10.$$

$$\sigma_{\phi,m} = N_\phi/h \quad \sigma_{\theta,m} = N_\theta/h \qquad 11.$$

$$\sigma_{\phi,B} = 6M_\phi/h^2 \quad \sigma_{\theta,B} = 6M_\phi/h^2 \qquad 12.$$

where

$$D = Eh^3/12(1-\gamma^2) \quad ,$$

$$K = N_\alpha \sin^2\alpha + Q_\alpha \sin\alpha\cos\alpha \quad ,$$

and C_o is a constant of integration.

The subscripts m and B designate membrane and bending, respectively.

TABLES OF FUNCTIONS FOR THE CLASSICAL THEORY

Tables of values for the various series appearing in equations 3 to 12 were evaluated for 5 deg intervals from 5° to 45°.

It should be noted that the hypergeometric series z_1 and z_2 are convergent for $x = \sin^2\phi < 1$. Hence the degree of convergence is dependent upon the value of ϕ and δ (ratio a/h and γ).

For $a/h = 25$ and $\gamma = 0.3$ it was found that seventeen terms were needed in each series in order to obtain an accuracy of five significant figures.

The following tables of values are included in this report:

Table I - Q and $Q\cot\phi$

Table II - Q' and V

Table III - M_ϕ and M_θ .

RESULTS

Having the tables of values, one needs then to solve for the four constants of integration C_j, by the conditions at the edges. These then, in turn, are substituted back into the various expressions (equations 5 to 12) to obtain the desired results.

Case I - General Loading

For the case of general loading the edge conditions are

$$\text{at } \phi = 5^\circ \quad N_\phi = N_\alpha \quad Q = Q_\alpha \quad \text{and} \quad M_\phi = M_\alpha$$

$$\text{at } \phi = 45^\circ \quad Q = Q_\beta \quad \text{and} \quad M_\phi = M_\beta \quad .$$

The constant of integration, C_o, for equations 9 and 10 was determined by setting the tangential displacemnt at the outer edge, v_β, equal to zero.

The radial deflections, w, for each of the independent loads, N_α, Q_α, Q_β, and M_β are shown in Figs. 2a, b, c, d, and e.

The tangential displacement at the inner edge, v_α, is

$$v_\alpha/h = (0.039Q_\alpha - 2.840N_\alpha - 4.0193Q_\beta)/Eh \qquad 13.$$

The membrane and bending stresses are shown in Figs. 3 to 10, inclusive.

TABLE I

Q and Q cot ϕ

$a/h = 25 \qquad \gamma = 0.3$

$Q = C_1Q_1 + C_2Q_2 + C_3Q_3 + C_4Q_4 \qquad Q \cot \phi$

ϕ Degrees	Q_1	Q_2	Q_3	Q_4	$Q_1 \cot \phi$	$Q_2 \cot \phi$	$Q_3 \cot \phi$	$Q_4 \cot \phi$
5	.08706	-.00686	-.34373	.5923	.9951	-.07842	-3.928	6.770
10	.16856	-.05460	-.40865	.49618	.95595	-.30967	-2.3176	2.8140
15	.21764	-.18016	-.26308	.75170	.81225	-.67248	-.98184	2.8054
20	.16746	-.40089	.23668	1.1275	.46010	-1.1014	.65028	3.0978
25	-.09555	-.67733	1.2723	1.3120	-.20491	-1.4525	2.7284	2.8136
30	-.70533	-.8517	2.8901	.730	-1.2217	-1.4752	5.0059	1.26
35	-1.72213	-.57885	4.6800	-1.4741	-2.4594	-.82901	6.6835	-2.1036
40	-2.9342	.69484	5.3040	-6.1741	-3.4970	.82811	6.3213	-7.3583
45	-3.5467	3.5853	2.053	-13.454	-3.5467	3.5853	2.053	-13.454

TABLE II

Q'and V

$a/h = 25 \quad \gamma = 0.3$

$Q' = C_1Q_1' + C_2Q_2' + C_3Q_3' + C_4Q_4'$ $\qquad$ $V\frac{Eh}{d} = C_1V_1 + C_2V_2 + C_3V_3 + C_4V_4$

ϕ Degrees	Q_1'	Q_2'	Q_3'	Q_4'	V_1	V_2	V_3	V_4
5	.98874	-.23577	-1.7324	-5.2378	-.5407	-7.194	48.83	28.57
10	.83161	-.93164	.2833	1.4906	-4.4605	-13.941	40.868	33.909
15	.16739	-1.9859	3.3436	4.0274	-14.819	-18.034	62.022	21.960
20	-1.5383	-3.0096	8.4879	4.0187	-33.069	-13.955	93.218	-19.215
25	-4.7621	-3.0396	15.396	-.8816	-55.986	7.691	108.77	-104.72
30	-9.3590	-.3048	20.984	-14.133	-70.574	58.014	61.2	-238.54
35	-13.586	7.6377	17.552	-38.197	-48.338	142.10	-120.3	-387.07
40	-12.731	22.813	-8.420	-69.969	56.524	242.20	-508.48	-440.03
45	1.9253	44.003	-74.043	-92.983	295.14	294.09	-1110.9	-173.6

TABLE III

M_ϕ and M_θ

$a/h = 25 \quad \gamma = 0.3$

$$\frac{-273\ M_\phi}{h} = C_1 M_{\phi 1} + C_2 M_{\theta 2} + C_3 M_{\theta 3} + C_4 M_{\theta 4} \quad (*)$$

$$\frac{-273\ M_\theta}{h} = C_1 M_{\theta 1} + C_2 M_{\theta 2} + C_3 M_{\theta 3} + C_4 M_{\theta 4} \quad (**)$$

ϕ Degrees	$M_{\phi 1}$	$M_{\phi 2}$	$M_{\phi 3}$	$M_{\phi 4}$	$M_{\theta 1}$	$M_{\theta 2}$	$M_{\theta 3}$	$M_{\theta 4}$
5	-21.035	-106.42	-265.8	239.53	-11.93	-106.76	428.1	369.1
10	-84.306	-92.701	192.73	34.74	-48.312	-99.759	268.72	185.43
15	-180.60	-34.62	403.16	-250.43	-104.51	-71.633	331.59	-.549
20	-276.35	114.69	411.39	-715.85	-165.58	-.484	356.49	-262.79
25	-288.56	397.46	1.76	-1339.6	-195.82	134.24	212.80	-606.23
30	-64.66	803.24	-1129.5	-1861.7	-130.64	332.42	-242.0	-934.51
35	606.19	1185.6	-3202.1	-1627.3	119.04	540.34	-1117.0	-991.22
40	1901.1	1145.2	-5964.7	517.3	631.63	606.23	-2340.9	-322.05
45	3724.4	-57.63	-8037.2	6037.0	1385.9	250.33	-3422.1	1653.1

$$*M_{\phi,j} = -\frac{D}{a^2}\left[V_j \cot\phi + V_j'\right]$$

$$**M_{\theta,j} = -\frac{D}{a^2}\left[V_j' + \gamma V_j \cot\phi\right]$$

$j = 1, 2, 3, 4$

UNCLASSIFIED
ORNL-LR-DWG. 16876

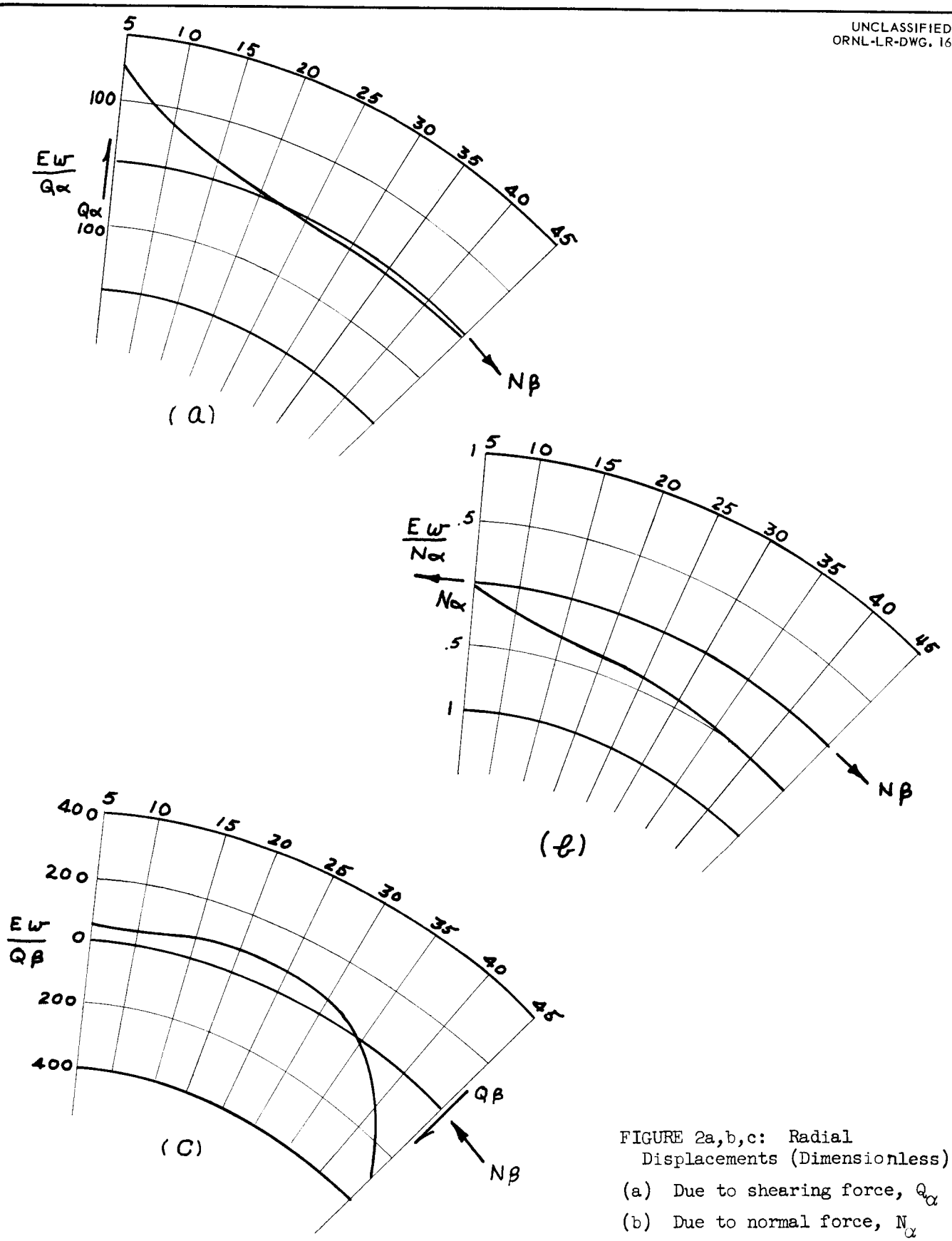

FIGURE 2a,b,c: Radial Displacements (Dimensionless)

(a) Due to shearing force, Q_α

(b) Due to normal force, N_α

(c) Due to shearing force, Q_β

UNCLASSIFIED
ORNL-LR-DWG. 16877

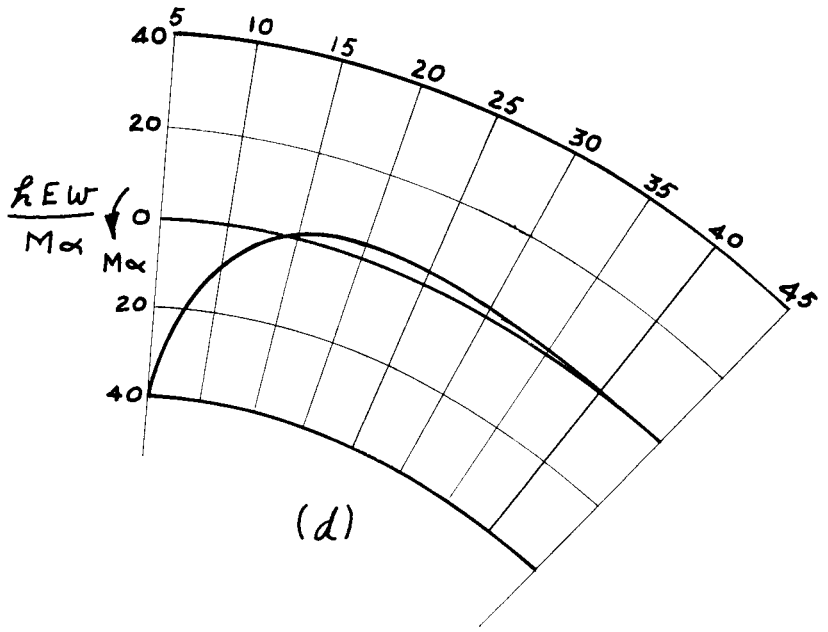

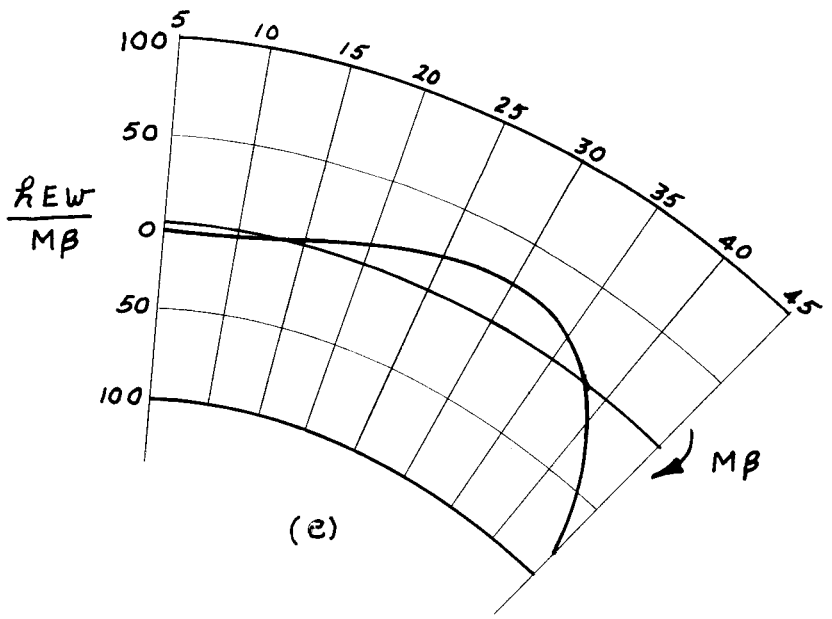

FIGURE 2d,e: Radial Displacements (Dimensionless)

(d) Due to bending moments, M_α

(e) Due to bending moments, M_β

UNCLASSIFIED
ORNL-LR-DWG. 16878

Meridional membrane stresses, $\sigma_{\phi,m}$, for Case I - General Loading; Figure 3, due to shearing forces Q_α and Q_β, Figure 4, due to normal force N_α and bending moments, M_α and M_β.

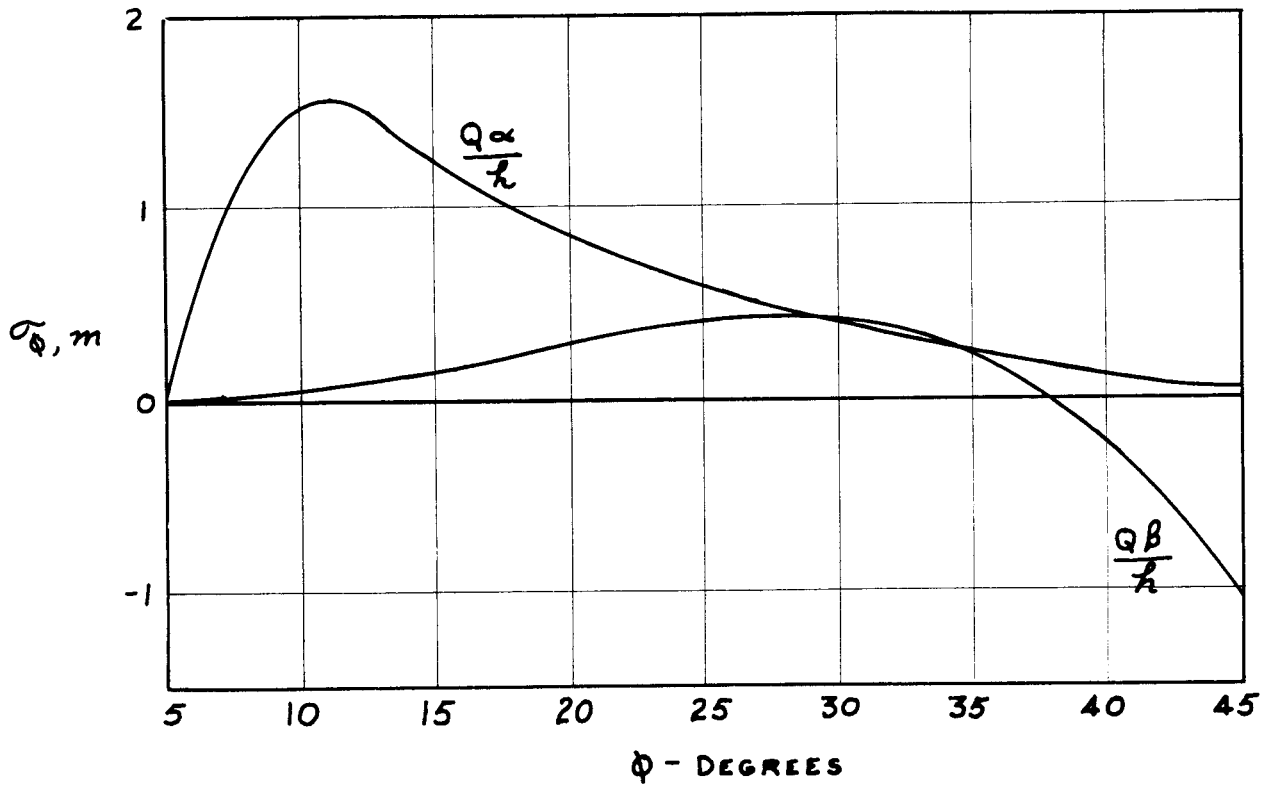

FIG. 3

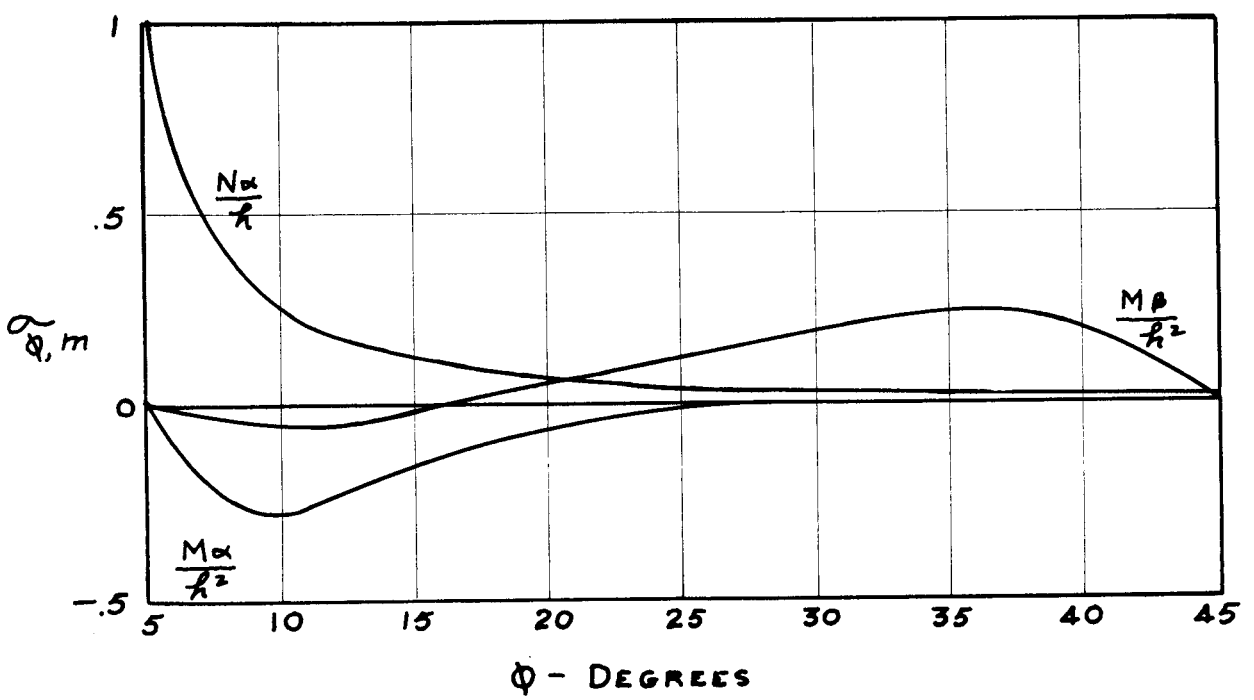

FIG. 4

UNCLASSIFIED
ORNL-LR-DWG. 16879

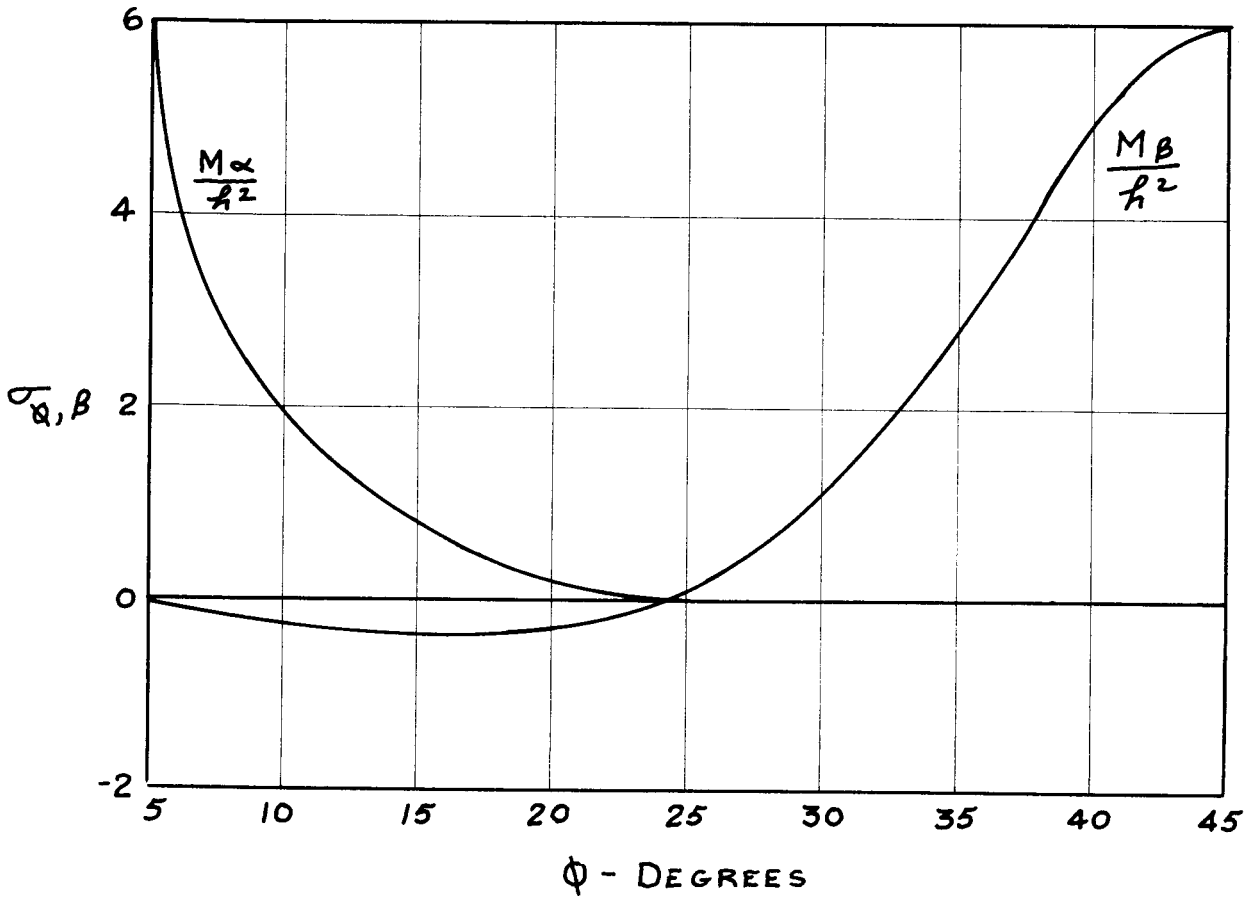

FIG. 5

Meridional bending stresses, outside surface, $\sigma_{\phi,B}$, for Case I - General Loading, due to bending moments, M_α and M_β.

UNCLASSIFIED
ORNL-LR-DWG. 16880

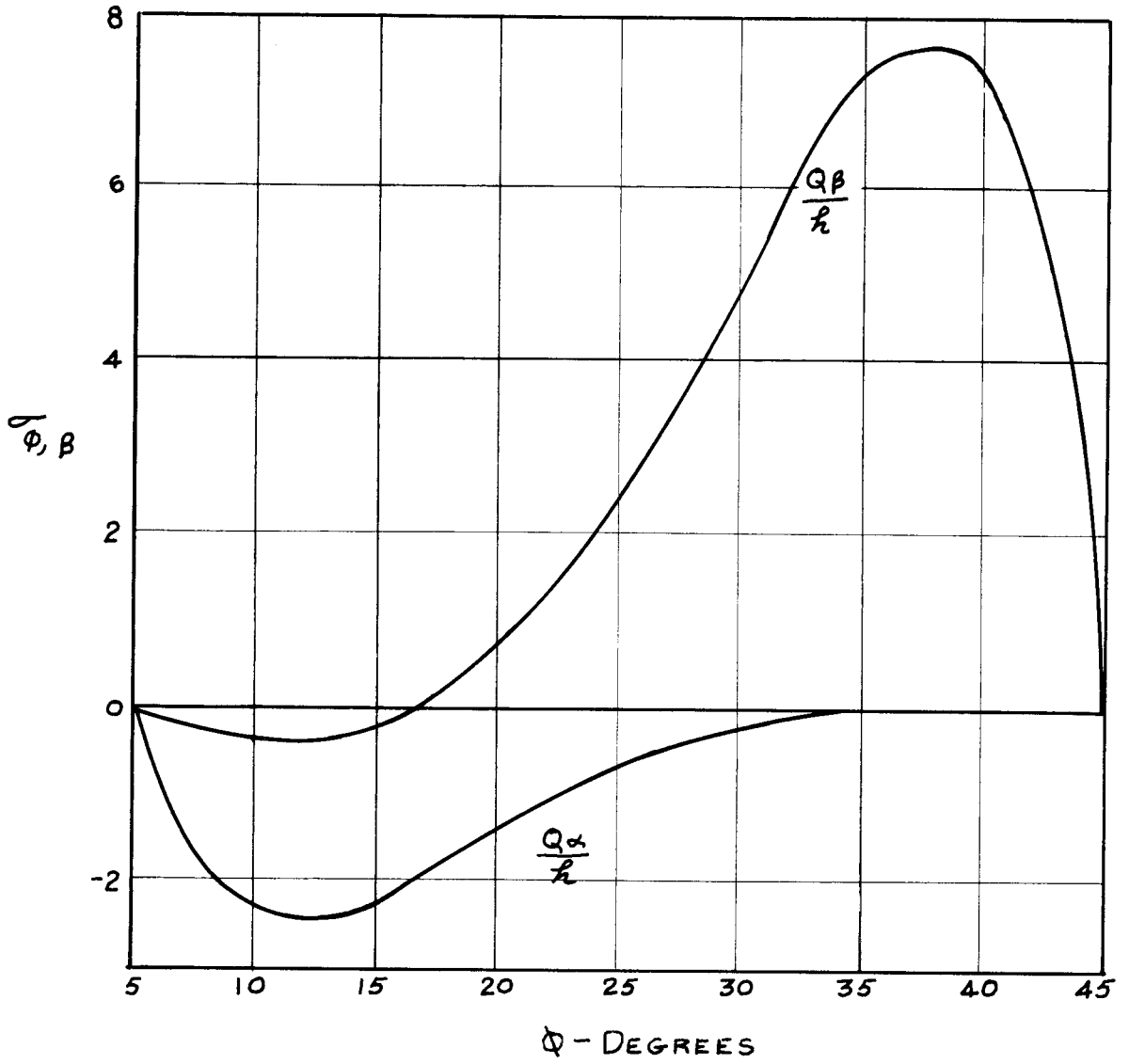

FIG. 6

Meridional bending stresses, outside surface, $\sigma_{\phi,B}$, for Case I - General Loading, due to shearing forces Q_α and Q_β.

UNCLASSIFIED
ORNL-LR-DWG. 16881

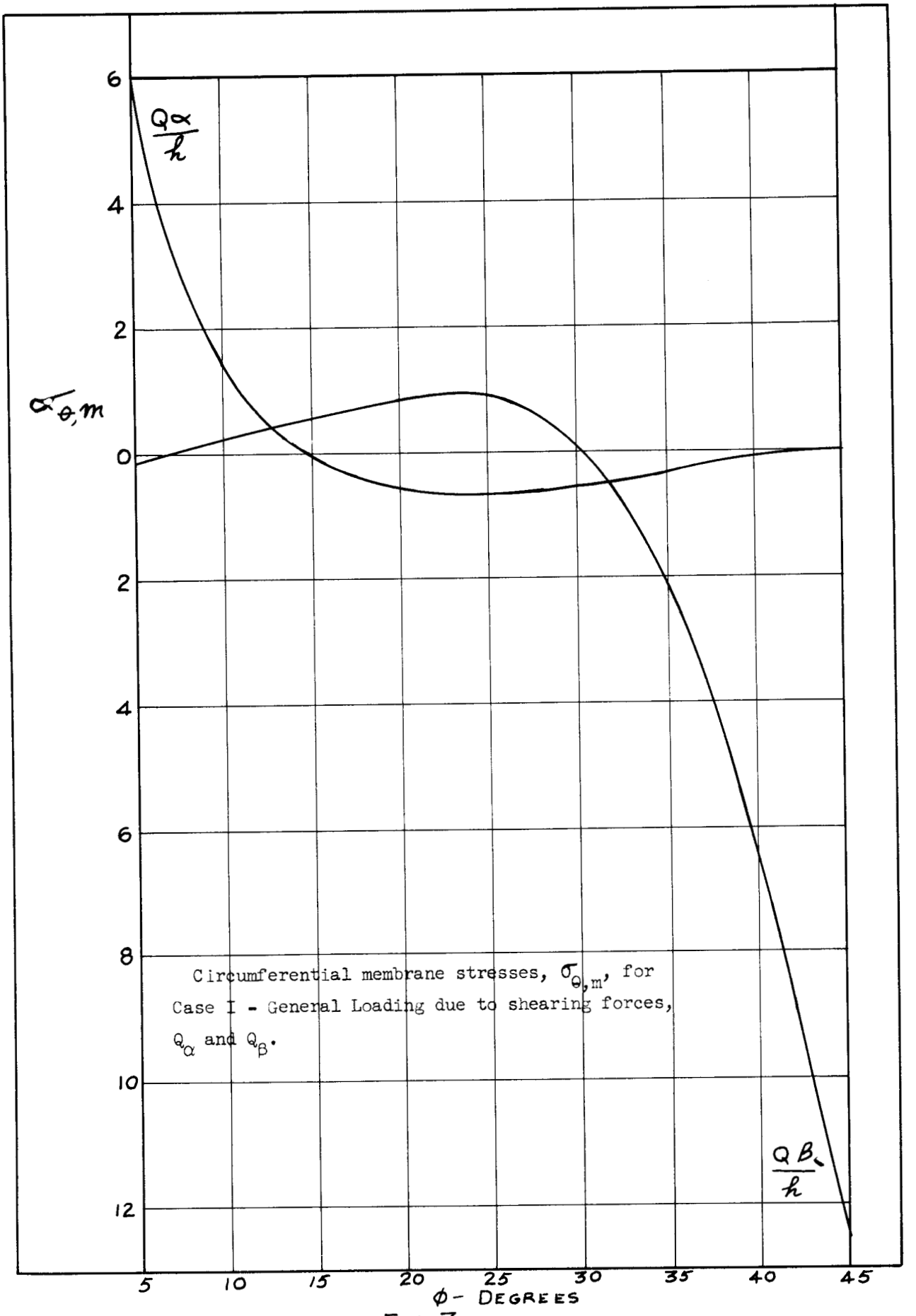

Circumferential membrane stresses, $\sigma_{\theta,m}$, for Case I - General Loading due to shearing forces, Q_α and Q_β.

FIG. 7

UNCLASSIFIED
ORNL-LR-DWG. 16882

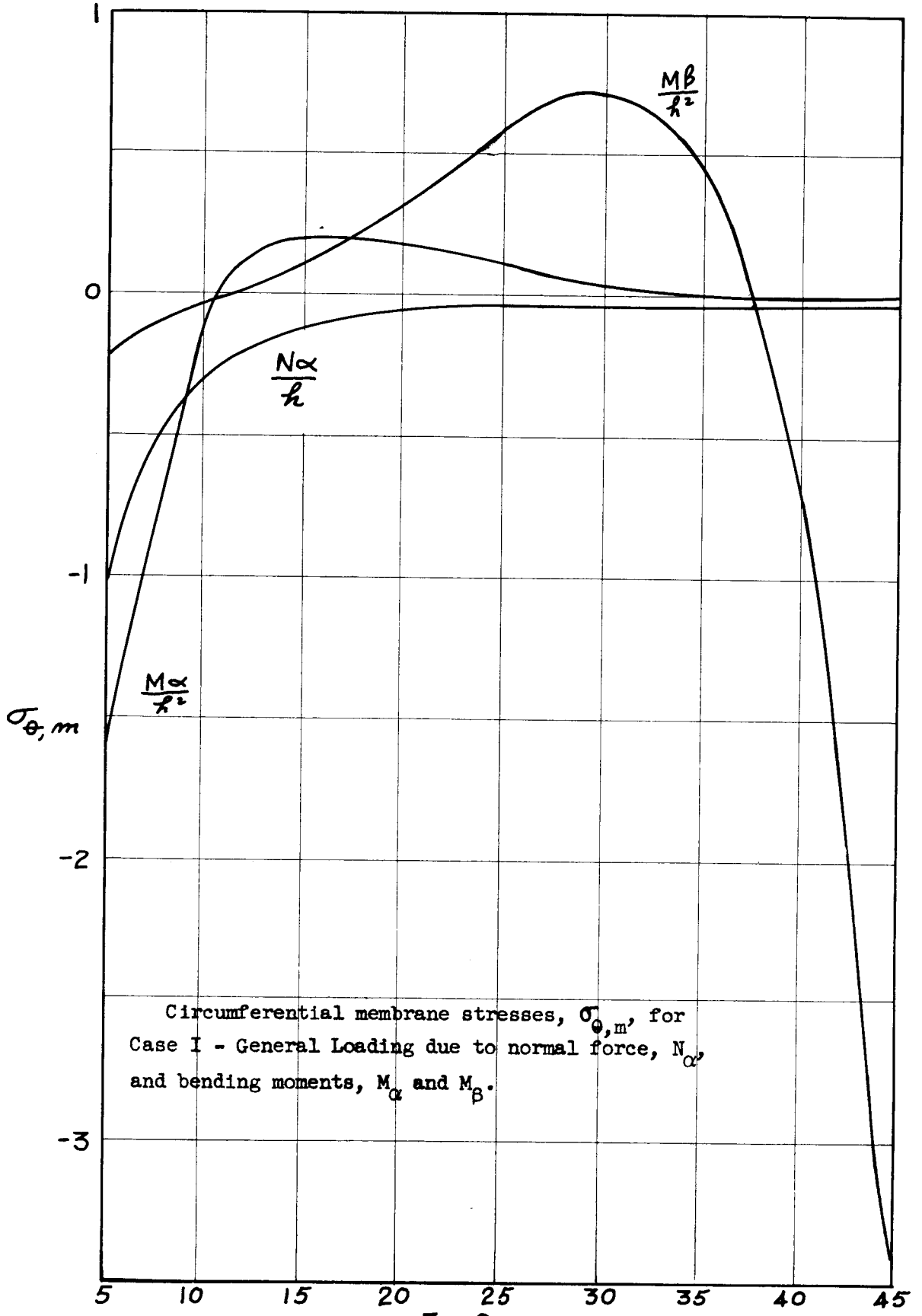

Circumferential membrane stresses, $\sigma_{\theta,m}$, for Case I - General Loading due to normal force, N_α, and bending moments, M_α and M_β.

FIG. 8

UNCLASSIFIED
ORNL-LR-DWG. 16883

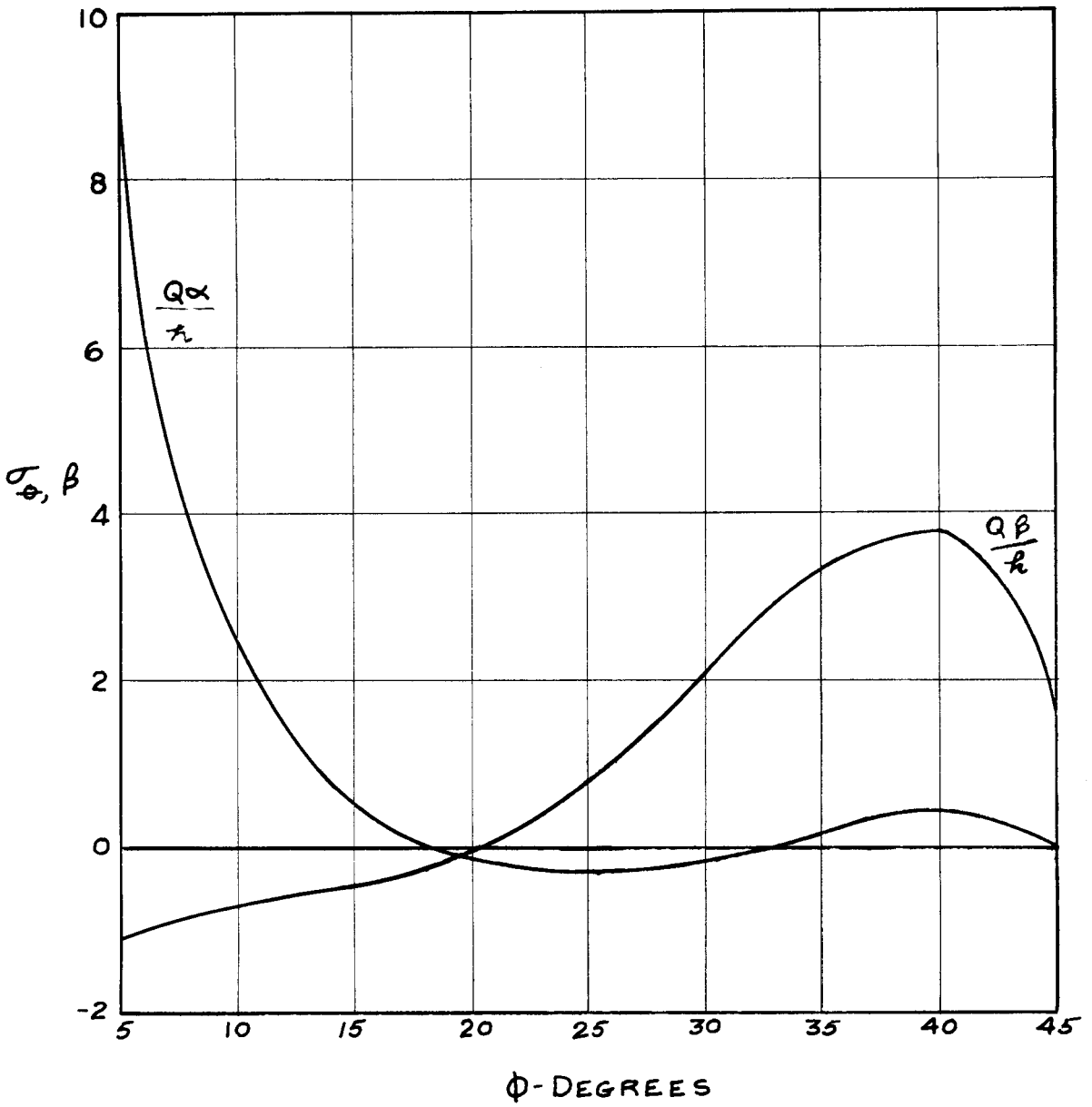

FIG. 9

Circumferential bending stresses, outside surface, $\sigma_{\theta,B}$, for Case I - General Loading due to shearing forces, Q_α and Q_β.

UNCLASSIFIED
ORNL-LR-DWG. 16884

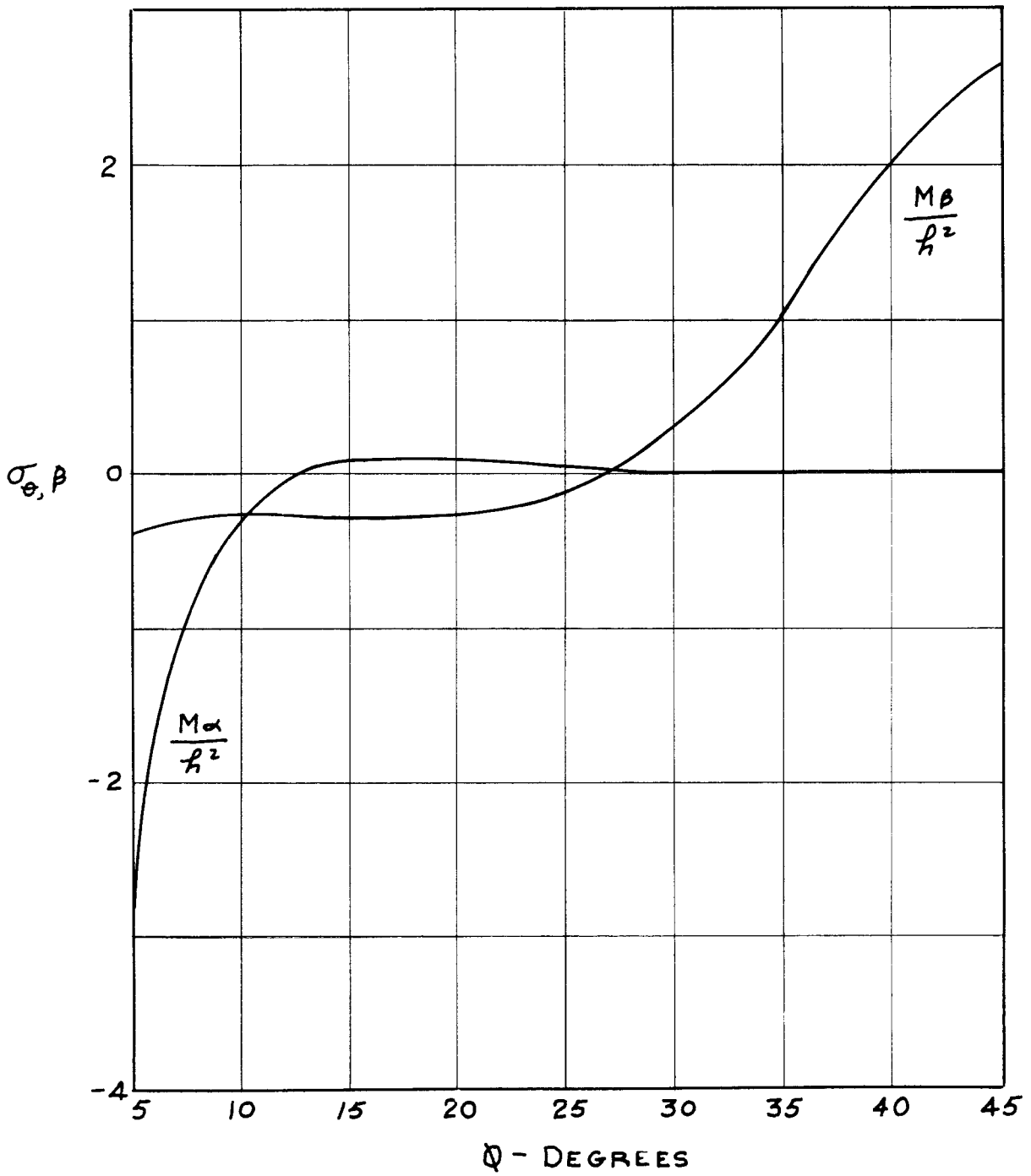

FIG. 10

Circumferential bending stresses, outside surface, $\sigma_{\theta,B}$, for Case I - General Loading due to bending moments, M_α and M_β.

Case II - General Loading at Inner Edge and Fixed at Outer Edge

The edge conditions for this case are

at $\phi = 5^{\circ}$ $N_{\phi} = N_{\alpha}$, $Q = Q_{\alpha}$ and $M_{\phi} = M_{\alpha}$

at $\phi = 45^{\circ}$ $V + w' = v = 0$ and $\epsilon_{\theta} = (N_{\theta} - \gamma N_{\phi})/Eh = 0$

C_o was evaluated by again taking $v_{\beta} = 0$.

The radial deflections, w, for Case II are shown in Fig. 11.

The membrane and bending stresses are shown in Figs. 12 to 15, inclusive.

The tangential displacement at the edge of the hole, v_{α}, was found to be

$$v_{\alpha}/h = (0.22\ Q_{\alpha} - 2.8412\ N_{\alpha})/Eh \qquad 14.$$

The reactions at the fixed edge were found to be

$$Q_{\beta} = 0.045\ Q_{\alpha} + 0.000268\ N_{\alpha} \qquad 15.$$

$$N_{\beta} = 0.214\ Q_{\alpha} + 0.01865\ N_{\alpha} \qquad 16.$$

$$M_{\beta} = (k)hQ_{\alpha} - 0.023\ M_{\alpha} + 0.006825\ hN_{\alpha} \qquad 17.$$

It was not possible to retain sufficient accuracy to evaluate (k), in equation 17, however, it can be stated that

$$-0.2 \leqslant k \leqslant 0.$$

UNCLASSIFIED
ORNL-LR-DWG. 16894

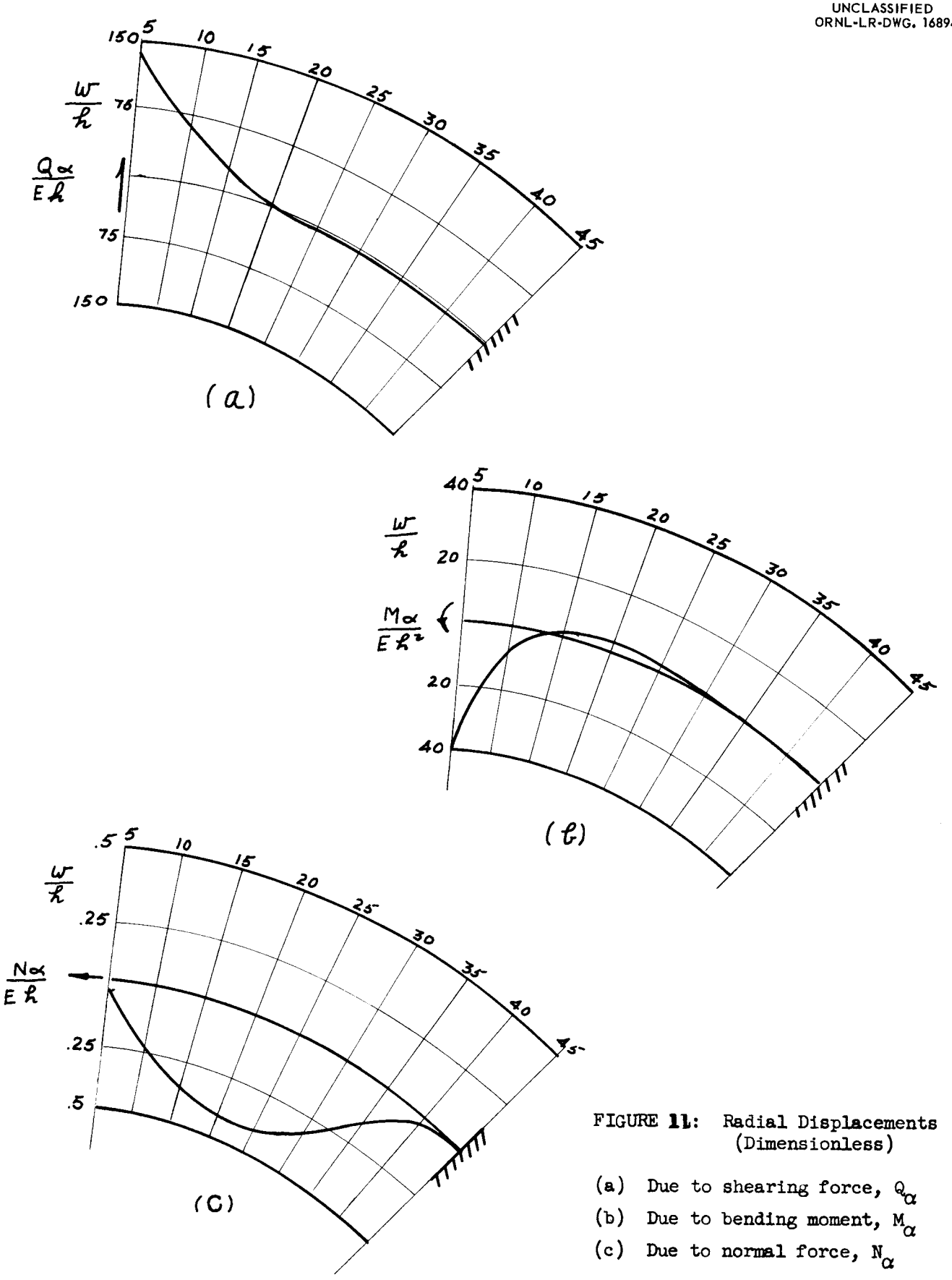

FIGURE 11: Radial Displacements (Dimensionless)

(a) Due to shearing force, Q_α

(b) Due to bending moment, M_α

(c) Due to normal force, N_α

UNCLASSIFIED
ORNL-LR-DWG. 16885

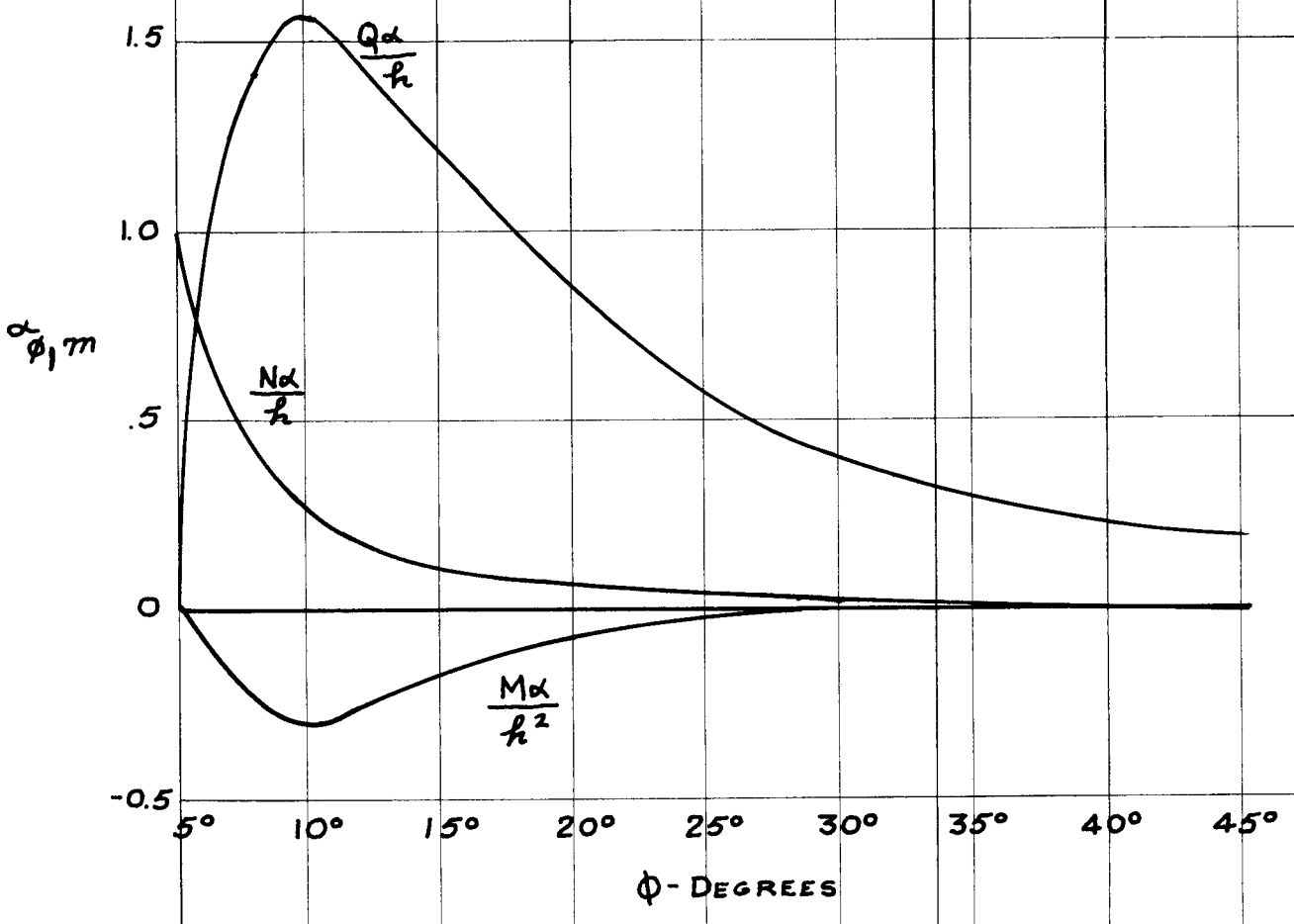

Figure 12

Meridional membrane stresses, $\sigma_{\theta,m}$, For Case II - Fixed Outer Edge, due to loads applied at inner edge.

UNCLASSIFIED
ORNL-LR-DWG. 16886

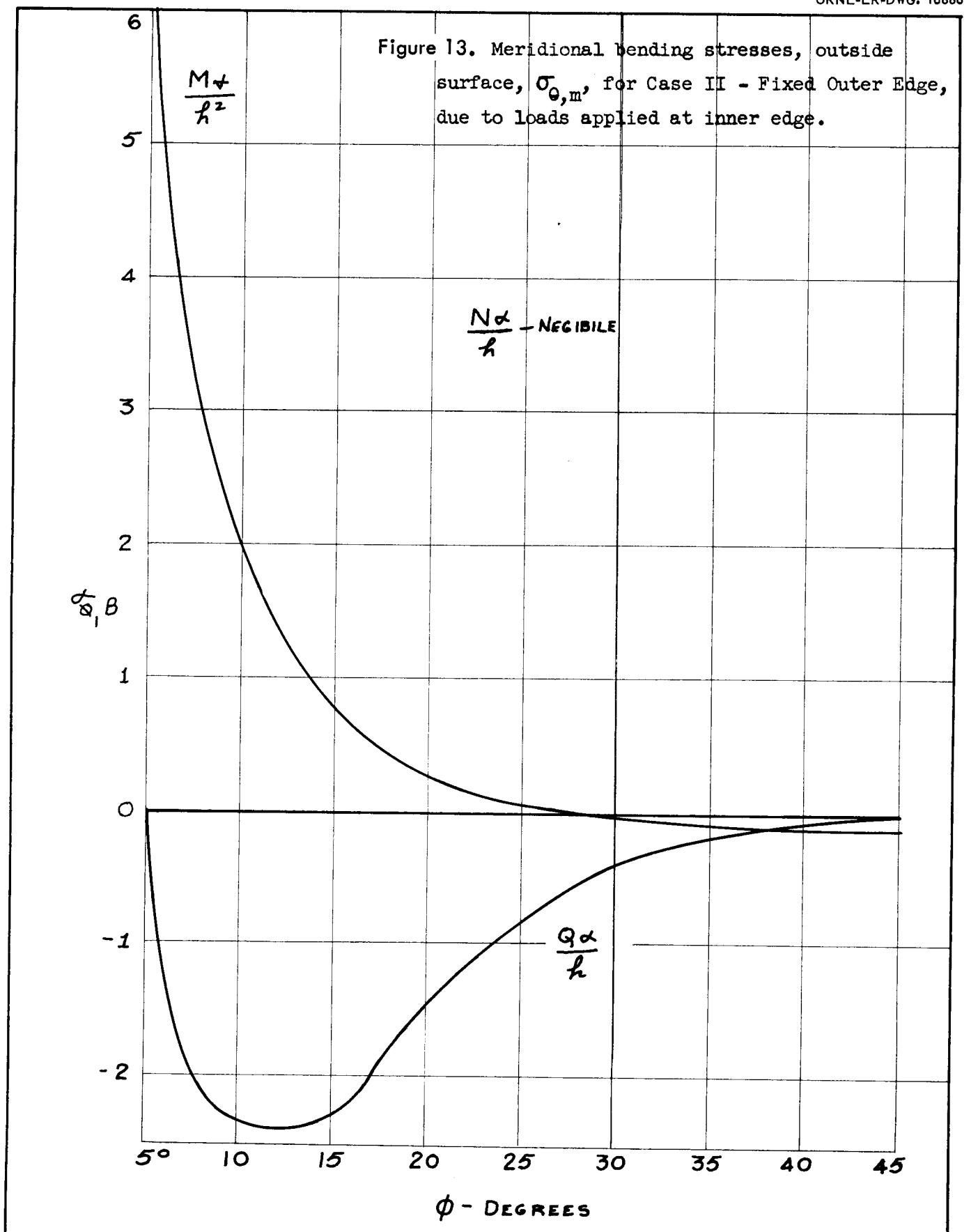

Figure 13. Meridional bending stresses, outside surface, $\sigma_{\theta,m}$, for Case II - Fixed Outer Edge, due to loads applied at inner edge.

UNCLASSIFIED
ORNL-LR-DWG. 16887

Figure 14. Circumferential membrane stresses, $\sigma_{\theta,m}$, for Case II - Fixed Outer Edge, due to loads applied at inner edge.

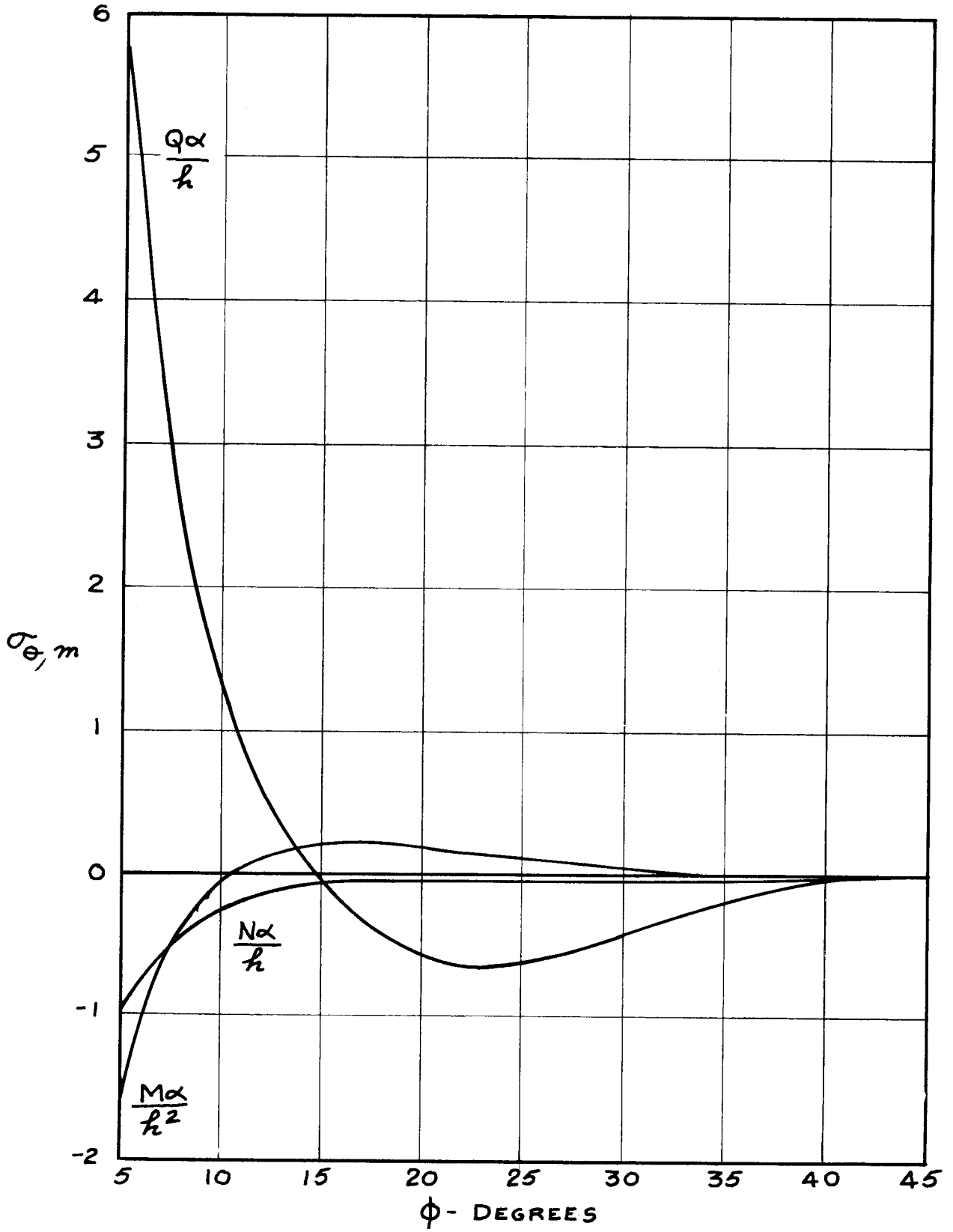

UNCLASSIFIED
ORNL-LR-DWG. 16888

Figure 15. Circumferential bending stresses, outside surface, $\sigma_{\theta,B}$, for Case II - Fixed Outer Edge, due to loads applied at inner edge.

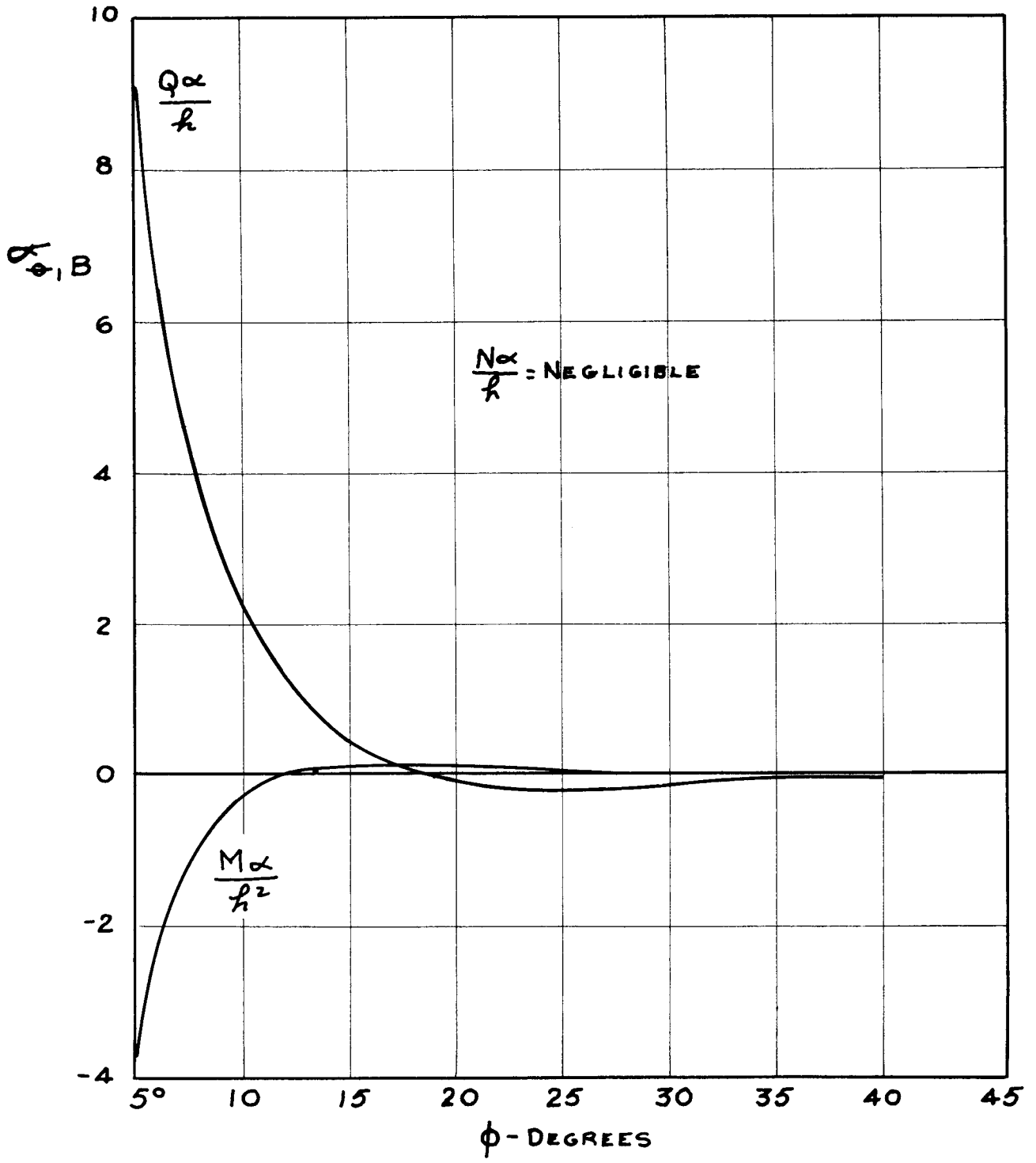

DISCUSSION OF RESULTS

It is generally known that stresses produced by loads applied along a circular hole (inner edge) of a spherical shell die out rather rapidly away from the hole. The results of this paper bear this out.

On the other hand, it is not strictly correct to say that stresses near the hole produced by loads at the outer edge are neglibible, even though they are smaller than the stresses produced in the vicinity of the outer edge. It is noted, however, if this outer edge is a supporting edge, such as in Case II, these stresses are negligible. This is substantiated by the results for Case II (Equations 15, 16, and 17).

It was found, for $\alpha = 5^{\circ}$ and $\beta = 45^{\circ}$, that considerable accuracy was lost in solving the set of simultaneous equations, necessary to obtain the constants of integration C_j. For these particular values of α and β, it is desirable to have the original series evaluated to more than five significant figures.

In considering the stresses produced by the shearing forces, Q_α and Q_β and the normal force, N_α, it may be helpful to point out that each one of these loads is held in equilibrium by a normal force at the outer edge, N_β.

CONCLUSIONS

On the basis of the experience obtained in carrying out the numerous numerical work and the results presented in this paper, the following conclusions appear warranted:

1. Convergence of the original series for Q is very slow for values of $\phi > 45^{\circ}$.

2. Evaluation of the series must be carried out to at least five significant figures. More accuracy is desired, particularly for small values of α.

3. If the critical loads are applied at the inner edge and the outer edge acts primarily as a "supporting edge", the angle β may be reduced, say, around 35°. (Furthermore, it may be stated that the results are affected very little by the type of "support" assumed at the outer edge).

4. In viewing the results due to loads applied at the outer edge, one should exercise caution in extrapolating the results for different values of α and β.

APPENDIX A

AXIALLY LOADED CIRCULAR CYLINDER ATTACHED TO SPHERICAL SHELL

Procedure

We now consider a spherical shell with an axially loaded circular cylinder attached to the inner edge (See Fig. A1). We obtain Q_α, N_α, and M_α in terms of the axial load, P, with the following relationships:

$$Q_\alpha \cos_\alpha + N_\alpha \sin\alpha = P/2\pi r \qquad \text{(a)}$$

$$(w_o)_c = (w_o)_s \qquad \text{(b)}$$

$$\left.\frac{(dw_c)}{(dt)}\right|_{x=0} = \left.\frac{(dw_s)}{(ad\phi)}\right|_{\phi=\alpha} \qquad \text{(c)}$$

Equation (a) is simply an equation of equilibrium. Equations (b) and (c) equate the displacements and the slopes at the lower edge of the cylinder and the inner edge of the shell, respectively.

From the general theory of cylindrical shells, we have the following relations:

$$(w_o)_c = -\frac{1}{2\rho^3 D_c}\left(\rho M_\alpha + Q_o\right) \qquad \text{(d)}$$

$$\left.\frac{(dwc)}{(dx)}\right|_{x=0} = \frac{1}{2\rho^2 D_c}\left(2\rho M_o + Q_o\right) \qquad \text{(e)}$$

where $\rho^4 = \dfrac{3(1-\gamma^2)}{r^2 t^2}$ $\qquad D_c = \dfrac{Et^3}{12(1-\gamma^2)}$

t = thickness of cylinder

r = radius of middle surface of cylinder

UNCLASSIFIED
ORNL-LR-DWG. 16889

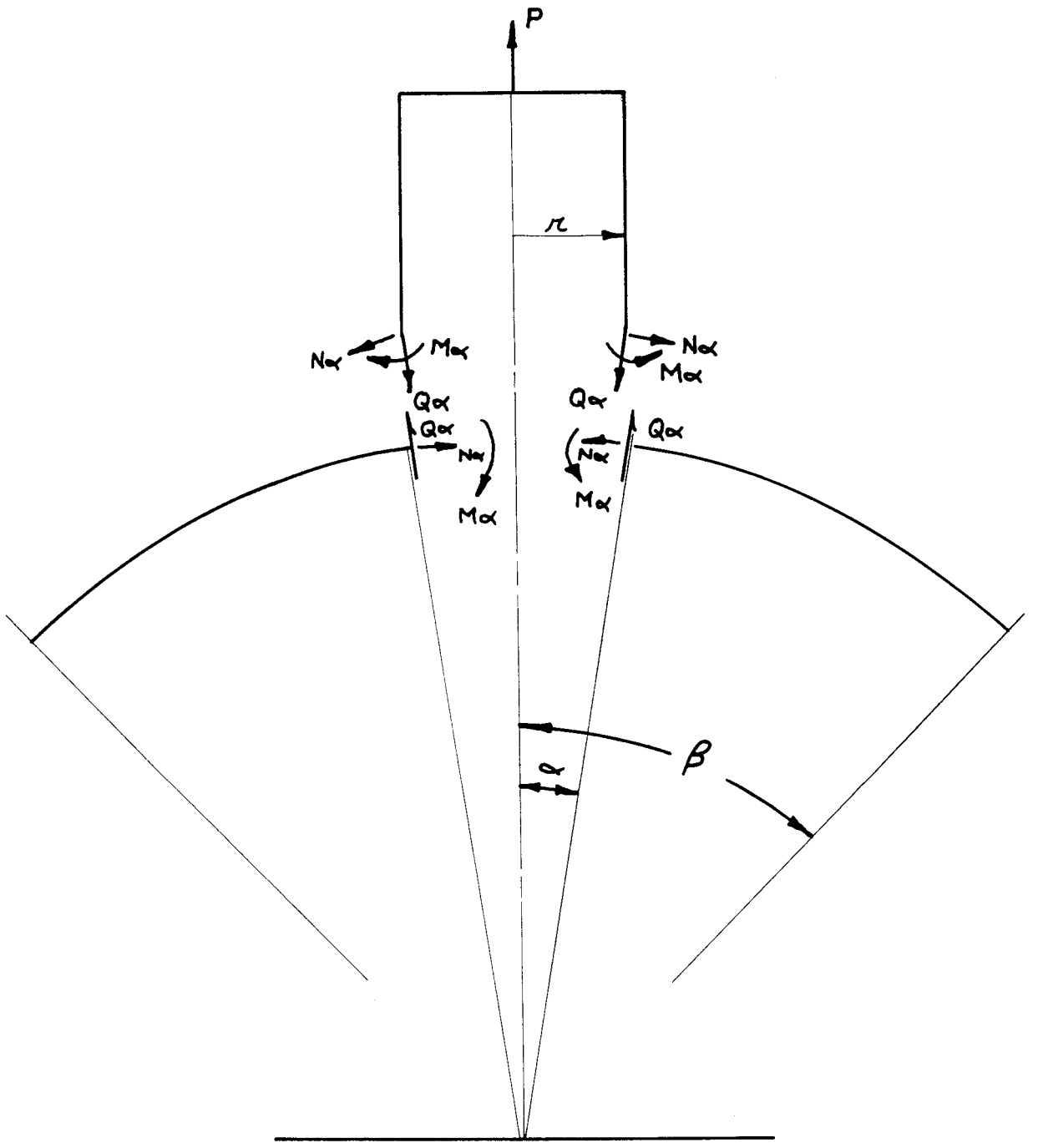

FIGURE A1

Axially loaded circular cylinder connected to spherical shell.

And Q_o = Horizontal (radial) force on lower edge of cylinder

$$= N_\alpha \cos_\alpha - Q_\alpha \sin_\alpha$$

The horizontal displacement at the inner edge of the shell, $(w_o)s$, is the sum of the horizontal components of the radial and tangential displacements at the inner edge, i.e.,

$$(w_o)_s = w_\alpha \sin_\alpha - v_\alpha \cos\alpha \qquad \text{(f)}$$

It can be shown that the slope at the inner edge of the shell is:

$$\frac{(dw)}{(ad\phi)}\phi = \alpha = \frac{1}{Eh}\Big[K\,(1+\gamma)(\cot\alpha - \sin\alpha \ln \tan\frac{\alpha}{2})$$

$$+ \left(\frac{-Q}{\sin^2\alpha} + Q'\cot\alpha + Q''\right) - C_o\,(1+\gamma)\sin\alpha\Big]$$

Thus, it is seen that the second derivative of the series for Q is needed. This was done for $\phi = 5^o$ and 10°, and the values are given in Table A1.

TABLE A1

Q"

ϕ Degrees	Q_1"	Q_2"	Q_3"	Q_4"
5	-0.32142	-5.4357	22.991	165.84
10	-3.5127	-10.726	25.212	42.414

RESULTS

Several cases of an axially loaded cylinder connected to a spherical shell were considered. The relative geometrical properties and edge condition at the outer edge for the several cases are summarized in Table A2. The values of the dimensionless, resulting loads $2\pi r Q_\alpha/h$, $2\pi r M_\alpha/Ph$, and $2\pi r N_\alpha/P$, at the junction of the shell and cylinder, for each case are summarized in Table A3.

TABLE A2

Summary of the Geometrical Dimensions for the Cases Considered

Geometrical Property	Test Model	Case A1	Case A2	Case A3	Case A4
α	3.4°	5°	5°	5°	10°
β	68.4°	45°	45°	45°	45°
Outer Edge Condition $\phi=\beta$	Fixed	Fixed	$Q_\beta=M_\beta=0$	Fixed	$Q_\beta=M_\beta=0$
r/t	1.599	1.599	1.599	4.663	7.19
h/t	1.014	1.014	1.014	3.84	2
a/h	26.51	25	25	25	25

TABLE A3

Partial Results

Dimensionless Load	Case A1	Case A2	Case A3	Case A4
$2\pi r Q\alpha/P$	0.9925	0.9919	0.9750	0.9455
$2\pi r M\alpha/Ph$	0.8475	0.8421	0.08086	0.3810
$2\pi r N\alpha/P$	0.1297	0.13488	0.3293	0.3966

CASE A1

The relative dimensions for this case coincide as nearily as it was possible to do so with those of a test model. The principal stresses at both the outside and inside surfaces were calculated and are plotted in Figs. A2 and A3. The corresponding experimental* stresses are also plotted on these figs. and are shown as enclosed dots. The results are for P = 2000 lb and r = 0.80. The scale for the dimensionless stress, $2\pi rh\sigma/P$, is shown as the right ordinate.

CASE A2

Case A2 is the same as Case A1 except for the outer edge condition. In Case A1 it was fixed and in Case A2, $Q_\beta = M_\beta = 0$.

The results for Case A2 are of very minor difference from Case A1 as indicated in Table A3. The principal stresses were calculated and it was found that they were within 150 psi of Case A1, and hence are not included in this report.

CASE A3

Case A3 differs from Case A1 only in the r/t and h/t ratios. The results for the dimensionless loads at the junction are shown in Table A3. The stresses were not calculated.

CASE A4

Case A4 differs substantially from the others in that the size of cylinder relative to the shell is larger ($\alpha = 10^\circ$). The r/t and h/t ratios are also different. $Q_\beta = M_\beta = 0$, at the outer edge. The principal dimensionless stress $2\pi r\sigma_{\phi,n}/P$ and $2\pi rh\sigma_{\theta,n}/P$, were calculated and are plotted in Figs. A4 and A5, respectively.

---

* The experimental results were obtained from a personal comminque to the author from Professor R. L. Maxwell, College of Engineering, University of Tennessee.

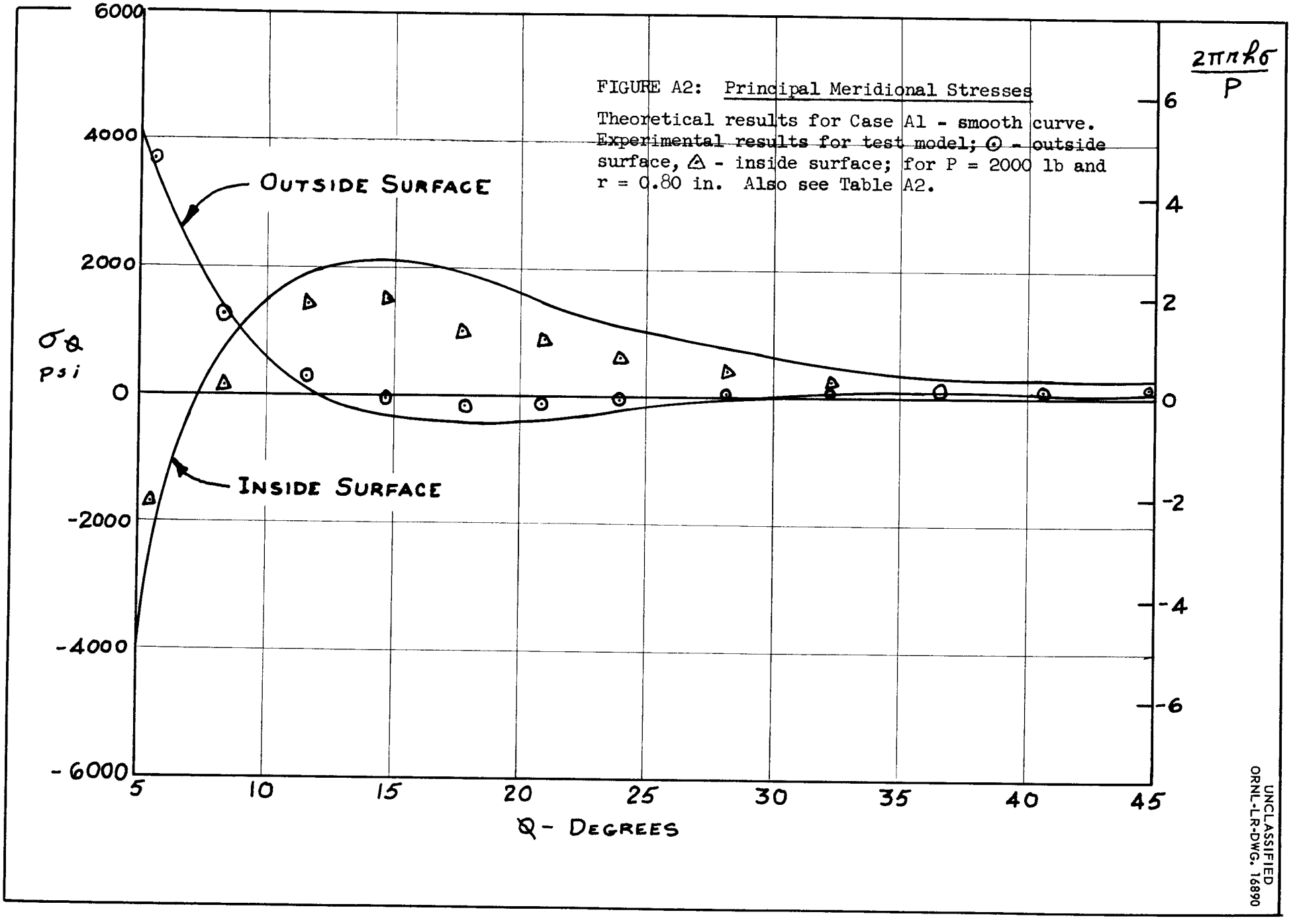

FIGURE A2: Principal Meridional Stresses

Theoretical results for Case A1 - smooth curve. Experimental results for test model; ⊙ - outside surface, △ - inside surface; for P = 2000 lb and r = 0.80 in. Also see Table A2.

UNCLASSIFIED
ORNL-LR-DWG. 16890

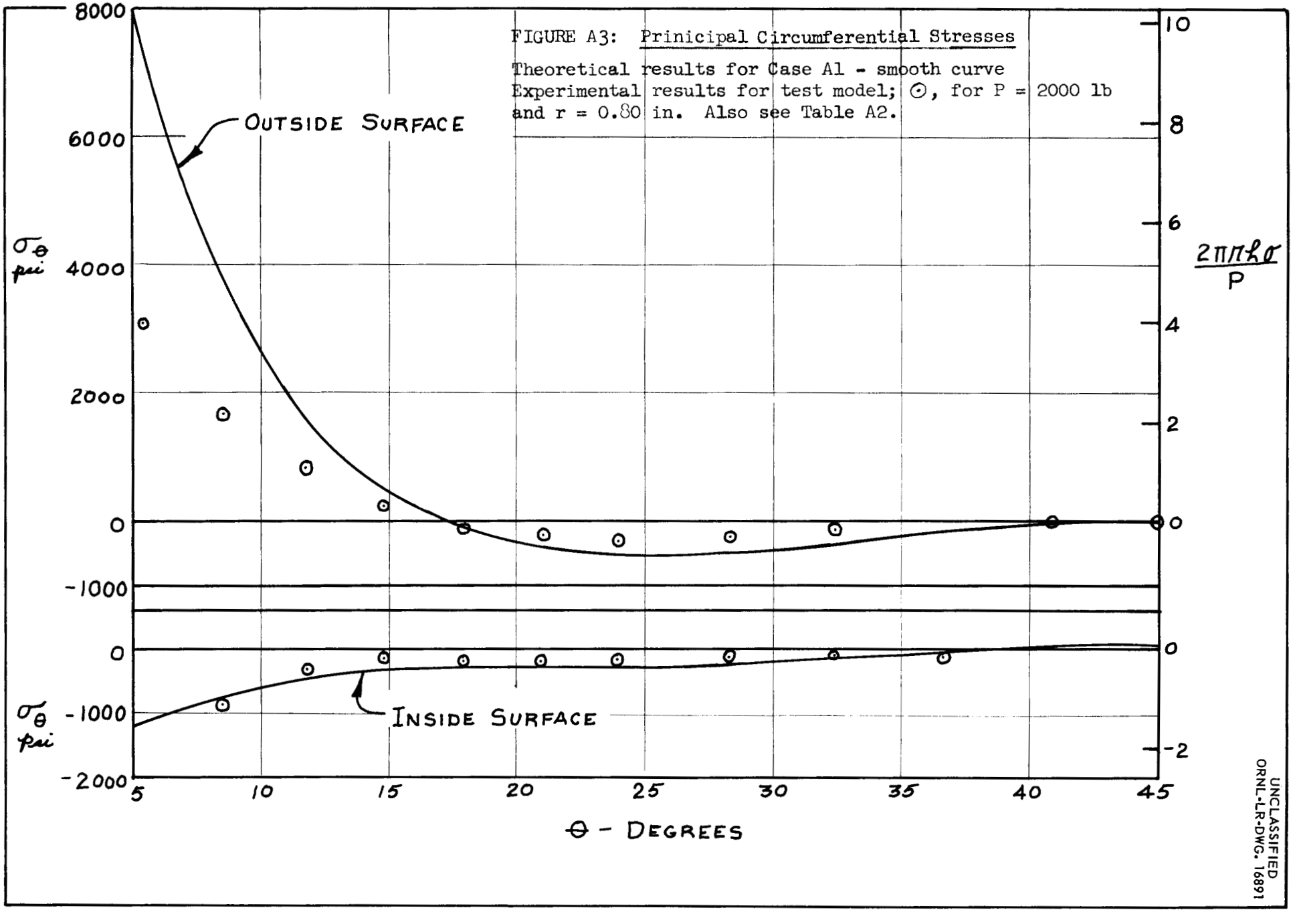

FIGURE A3: Prinicipal Circumferential Stresses

Theoretical results for Case A1 - smooth curve
Experimental results for test model; ⊙, for P = 2000 lb and r = 0.80 in. Also see Table A2.

UNCLASSIFIED
ORNL-LR-DWG. 16891

FIGURE A4: Principal Meridional Stresses for Case A4, see Table A2.

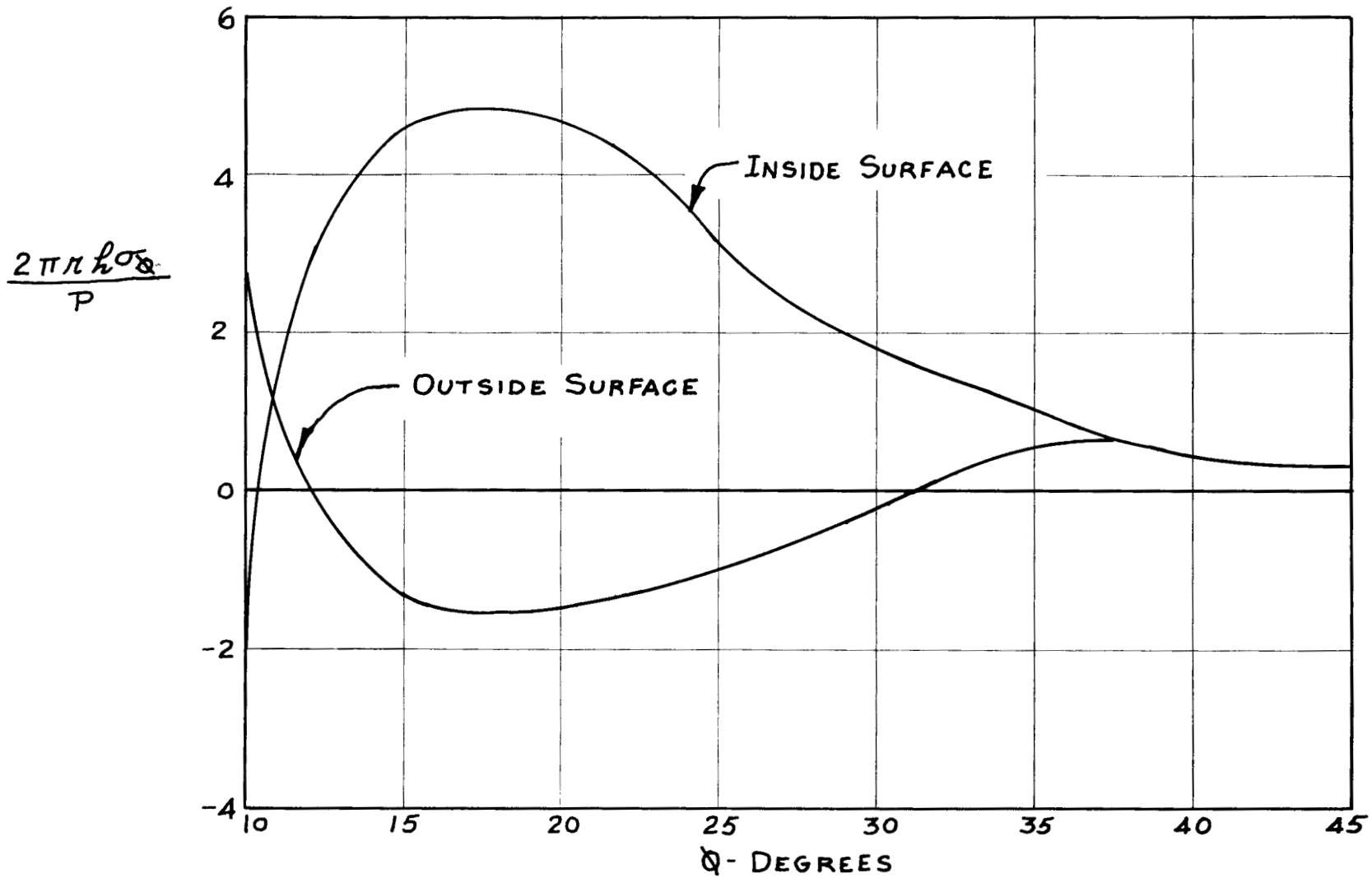

UNCLASSIFIED
ORNL-LR-DWG. 16892

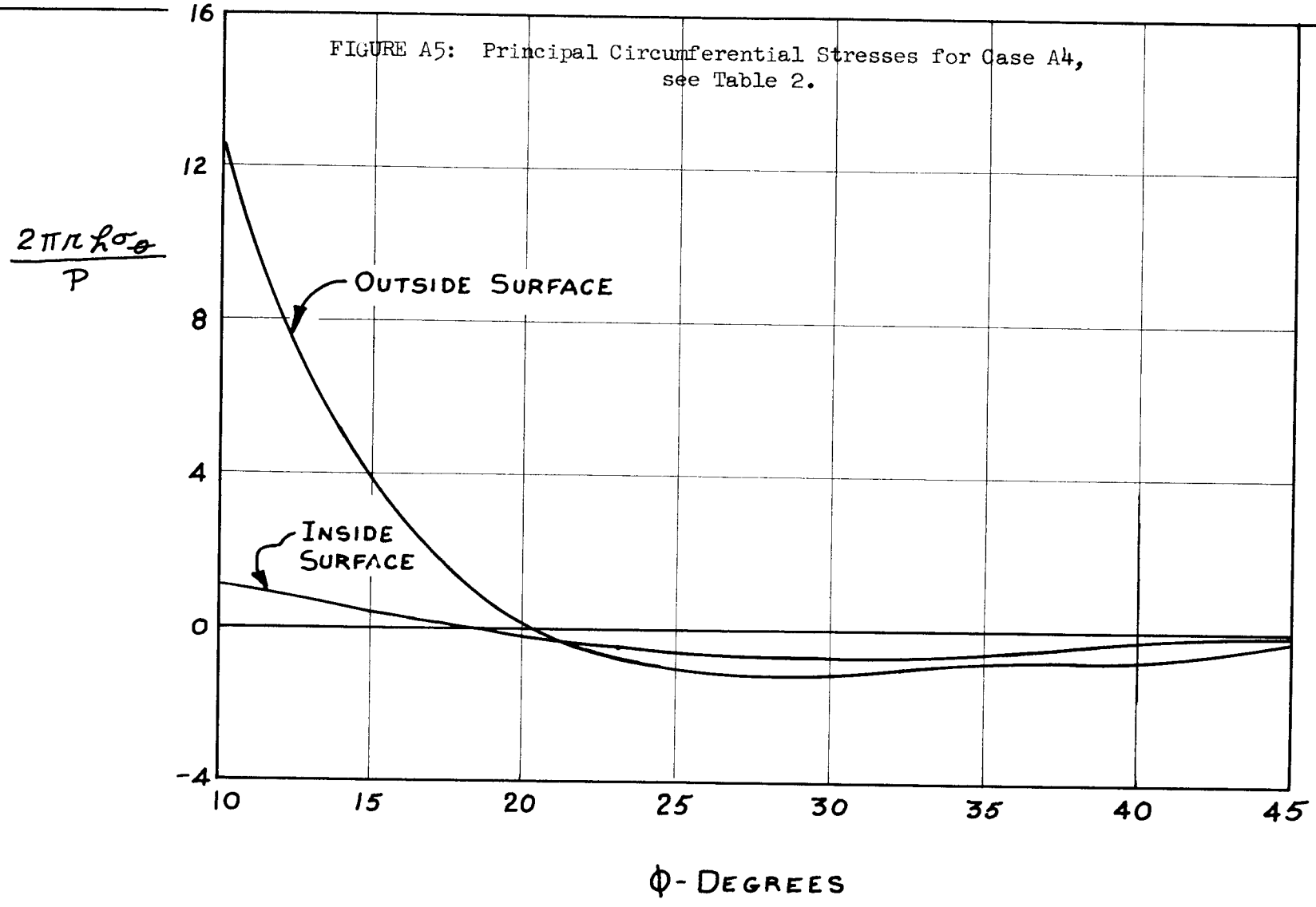

FIGURE A5: Principal Circumferential Stresses for Case A4, see Table 2.

UNCLASSIFIED
ORNL-LR-DWG. 16893

DISCUSSION OF RESULTS

A glance at Figs. A2 and A3 indicate a fair agreement between theoretical and experimental results. Before attempting to justify the differences which do exist, we make the following analyses, first:

A comparison of the results in Table A3 between Case A1 and A2, show that the outer edge condition has very minor influence upon the results. Hence, we may ignore that difference, for the moment, in this discussion.

In order to obtain intuitive exceptance of the other results in Table A3, several factors must be taken into account. Namely, α has changed in Case A4, and for Cases A3 and A4 the increase in the r/t ratio is partially offset by the decrease in the h/t ratio.

A comparison of Figs. A2 and A4 yield the following observations for the principal stresses in the meridional direction:

1. The stresses at the outside surface decrease as α is increased, i.e., the general shape of the curve shifts downward, as α is increased from 5° to 10°.
2. The stresses at the inside surface increase as α is increased; the general shape of the curve shifts upward, as α is increased from 5° to 10°.
   Similarly for the principal stresses in the circumferential direction by comparing Figs. A3 and A5.
3. The stresses at both the outside and inside surfaces, in the vicinity of α, increase as α is increased, i.e., the general shape of the curves, for $\alpha \leq \phi \lesssim 25^{\circ}$, shift upward.

To obtain intuitive exceptance of the above observations, it may be helpful to keep the following in mind:

(a) As α decreases, the condition in the vicinity of the inner edge of the shell approaches that of a circular hole in a flat plate.

(b) As α increases, this condition approaches that of a circular cylinder.

If we now pass an average smooth curve through the experimental points in Figs. A2 and A3, and then make a similar analysis as was done above, we would be led to the same three observations as those listed above. Hence, we conclude that in general, the major differences between the theoretical and experimental results in Figs. A2 and A3 are due primarily to the fact that α is of different magnitude in Case A1 and the test model.

It is noted in Fig. A4 that only membrane stresses exist in the vicinity of the outer edge, (the two curves coincide for $\phi \gtrsim 37.50^{\circ}$). This may be attributed to the fact that $Q_{\beta} = M_{\beta} = 0$ at the outer edge.

The maximum shearing stresses were not calculated. It may be noted, however, by comparing corresponding points in Figs. A2 and A3 (or A4 and A5) that the maximum shearing stress does not always occur on a plane normal to the sphere, 45° with the ϕ and θ direction, but rather on planes 45° with the normal to the surface.

CONCLUSIONS

For Appendix A the following conclusions appear appropriate:

1. There is very good agreement between theoretical and experimental results -- taking into account all of the physical differences between the models for which theoretical and experimental results were represented in this paper.

2. More accuracy was retained in solving for the constants of integration C_j, when $\alpha = 10^{\circ}$ than when $\alpha = 5^{\circ}$. See conclusion 2 from analysis of the spherical shell.

3. Conclusion 3 from the analysis of the spherical shell is further substantiated by the results represented in the appendix.

4. One should exercise caution in using approximation methods in which Q and/or $\frac{dQ}{d\phi}$ are neglected in the mathematical development of the theory, for an analysis of the problem considered in the appendix.